EXAMINING THE MARKERS OF VITAMIN C CYTOTOXICITY IN PANCREATIC DUCTAL ADENOCARCINOMA

by

Cassia Scarlett Warren

B.Sc., University of British Columbia (Vancouver), 2016

A THESIS SUBMITTED IN PARTIAL FULFILLMENT OF

THE REQUIREMENTS FOR THE DEGREE OF

MASTER OF SCIENCE

in

The Faculty of Graduate and Postdoctoral Studies

(Interdisciplinary Oncology)

THE UNIVERSITY OF BRITISH COLUMBIA

(Vancouver)

March 2019

The following individuals certify that they have read, and recommend to the Faculty of Graduate and Postdoctoral Studies for acceptance, a thesis/dissertation entitled:

Examining the markers of vitamin C cytotoxicity in pancreatic ductal adenocarcinoma

submitted by Cassia Warren in partial fulfillment of the requirements for

the degree of Master of Science

in Interdisciplinary Oncology

Examining Committee:

David Schaeffer
Supervisor

Janel Kopp
Supervisory Committee Member

Stephen Yip
Supervisory Committee Member

Rob Olson
Additional Examiner

Additional Supervisory Committee Members:

Daniel Renouf
Supervisory Committee Member

Supervisory Committee Member

Abstract

Pancreatic ductal adenocarcinoma (PDAC) remains one of the most lethal forms of cancer, with a 5-year survival rate of less than 10%. Current challenges include limited therapeutic options and lack of biomarkers that predict treatment response. Therefore, I sought to determine if a recently rediscovered treatment, pharmacological vitamin C, has clinical utility in PDAC. I determined that PDAC cell lines have differential sensitivity at doses tested. Previous research in colorectal cancer indicated that *KRAS* mutations infer vitamin C sensitivity, which was a trend in my results. Therefore, I created two isogenic cell line models expressing either *KRAS* G12D or *KRAS* G12V. Testing depicted increased sensitivity in one model but none others, suggesting that factors beyond oncogenic *KRAS* alone may be needed to increase sensitivity to vitamin C treatment.

Oncogenic *KRAS* is known to increase glycolysis through the Warburg effect. Interestingly, pharmacological vitamin C treatment is also hypothesized to affect this pathway. Therefore, I sought to determine the relationship between vitamin C and glycolysis to determine potential markers of vitamin C sensitivity. Testing glycolysis rates demonstrated that vitamin C inhibits glycolysis independent from vitamin C toxicity. Work by Daemen et al. identified that glycolytic inhibitors cause toxicity selective to glycolytic dependant cells, whereas lipogenic cells survive. Furthermore, they characterized our two vitamin C sensitive cell lines as glycolytic. To further understand if glycolytic dependence influences vitamin C sensitivity, I used glucose withdrawal to reduce the cell's glycolytic dependence. In low glucose conditions, higher doses of vitamin C were needed compared to high glucose conditions, suggesting that

glycolytic dependence does influence toxicity to vitamin C. Together, my results suggest that glycolytic dependence may be a good marker for determining vitamin C sensitivity.

To test if vitamin C is toxic in *KRAS* mutated patient-derived models, PDAC-derived organoids were created and treated using vitamin C monotherapy and combination therapy with gemcitabine. Vitamin C showed toxicity as a monotherapy and increased toxicity when combined with gemcitabine. This is the first known use of organoids in testing vitamin C treatment and suggests, congruent with other research, that vitamin C alone and in combination has clinical utility.

Lay Summary

Pancreatic cancer is a deadly disease that kills over five thousand Canadians a year and often patients succumb to their disease within a year. More treatment options and markers to tailor treatment decisions are urgently needed. High dose intravenous vitamin C has recently been shown to specifically kill certain types of cancer cells. Studies have suggested that this therapy inhibits glycolytic energy production and selectively targets colorectal cancer cells that have a *KRAS* mutation, a prevalent mutation in pancreatic cancer. I created a cell model system of pancreatic cancer that had either normal or mutant *KRAS*. This system identified that *KRAS* status may not be sufficient to predict sensitivity to vitamin C therapy. However, I identified that a high rate of glycolysis, often occurring in *KRAS* mutant cells, could be a marker of vitamin C sensitivity and may aid in determining which patients will benefit from this therapy.

Preface

Aims and experiments were developed and designed with guidance from Dr. Joanna Karasinska, Dr. Daniel Renouf, and Dr. David Schaeffer. Development, optimization, and testing of organoids were a joint effort between Dr. Joanna Karasinska, Andrew Metcalf, and myself. Western blots were executed by myself with the help of Hassan Ali. Seahorse glycolytic stress test was completed with assistance from Shawn Chafe. Genomic and transcriptomic data analysis of patient derived organoids was conducted by James Topham and Dr. Joanna Karasinska. All other experiments and all data analysis were conducted by myself.

Patient samples were obtained through the PANGEN project (NCT02869802) under BC Cancer ethics certificate H16-00291 and sequencing was completed by Canada's Michael Smith Genome Sciences Centre.

Table of Contents

List of Tables

List of Figures

List of Symbols and Abbreviations

2-DG	2-deoxy-D-glucose
5-FU	Fluorouracil
cg	Copy gain
COAD	Colorectal cancer
DHA	Dehydroascorbic acid
Dox	Doxycycline
ECAR	Extracellular Acidification Rate
FBS	Fetal bovine serum
GAPs	GTPase-activating proteins
Gem	Gemcitabine
GEPs	Guanine nucleotide exchange factors
GFP	Green fluorescent protein
GLUT1	Glucose transporter 1
GSH	Glutathione
GSSG	Oxidized Glutathione
H_2O_2	Hydrogen peroxide
HIF1- α	Hypoxia-inducible factor 1-alpha
ICGC	International Cancer Genome Consortium
IPMN	Intraductal papillary mucinous neoplasias
IV	Intravenous
LUAD	Lung adenocarcinoma
MEC	J28 #421 mouse epithelial cell line
MOI	Multiplicity of infection
mPDO	Metastatic patient-derived organoid
nd	Not determined
NTC	Non-targeting control
ORF	Open reading frame
OS	Overall survival
PanINs	Pancreatic intraepithelial neoplasia
PBS	Phosphate-buffered saline

PDAC	Pancreatic ductal adenocarcinoma
PDO	Patient-derived organoid
PNET	Pancreatic neuroendocrine tumour
RCT	Randomized Control Trial
ROS	Reactive Oxygen Species
rTA3	Tetracycline transactivator
TCGA	The Cancer Genome Atlas
TET	Ten-eleven translocation
TRE2	Tetracycline response element
xPDO	Xenograft patient-derived organoid

Acknowledgements

I would like to thank my supervisors Dr. Daniel Renouf and Dr. David Schaeffer for their mentorship, guidance, and support throughout my graduate studies. Thank you to my committee, Dr. Janel Kopp and Dr. Stephen Yip for your continuous constructive feedback. I especially would like to thank Dr. Joanna Karasinska for her intellectual and technical daily guidance and patience in answering my questions. Thank you to Hassan Ali, Andrew Metcalfe, Taixiang Wang, James Topham, and the rest of the Pancreas Centre Research team for your support. I would also like to thank Dr. Marcel Bally, Dr. Don Yapp, Wieslawa Dragowska, and the rest of the Experimental Therapeutics Department for their help and access to laboratory resources. And thank you to Francis Lynn for spending the time to teach me CRISPR.

Last but not least, a heartfelt thank you to my family, especially my parents, for their unconditional support and encouragement. Thank you to my friends and fellow classmates for their support and giving me incredible memories throughout graduate school.

Dedication

To my family

Chapter 1: Introduction

1.1 Pancreatic ductal adenocarcinoma

Pancreatic ductal adenocarcinoma (PDAC) is the 4th leading cause of cancer related death in Canada [1] and 3rd in the United States [2]. Pancreatic cancer has a lower incidence compared to other cancer types [1], however its 5-year survival rate is less than 10% [3], making it one of the deadliest forms of cancer. Furthermore, if outcomes are not improved, mortality rates are expected to double by 2030 due to increasing incidence [4], making PDAC the 2nd leading cause of cancer mortality in Canada [5].

Pancreatic cancer has two major subtypes, pancreatic ductal adenocarcinoma (PDAC) and pancreatic neuroendocrine tumours (PNETs). PNETs arise from endocrine cells in the pancreas that secrete insulin and glucagon hormones to regulate the metabolism of glucose; these tumours account for 5% of pancreatic cancers. Whereas, PDACs arise from exocrine cell types, ductal and acinar cells, and account for 95% of pancreatic cancers. The two subtypes not only differ in their cell of origin, but also in their mutational landscape, mortality rates, and treatment regimens [6-8]. This thesis focuses on the more common and lethal subtype, PDAC. The PDAC subtype is associated with major challenges in both its diagnosis and treatment, including late stage diagnosis and unresectable disease, limited benefit from current treatments, and lack of markers to predict treatment response.

1.1.1 Histology

Pancreatic ductal adenocarcinoma arises through the formation of intraepithelial neoplasias (PanIN) or intraductal papillary mucinous neoplasias (IPMN) [9-11]. Through the activation of multiple cancer promoting pathways, PanINs develop from low to high grade dysplasia [9]. When understanding the histology of PDAC, it is crucial to consider the

microenvironment; PDAC is known to harbour up to 90% stroma which heavily interacts with the cancer cells [12-14]. PDAC cells can release cytokines to promote stroma activation, but also activated stroma can lead to increased invasive activity of the cancer [15]. Moreover, having activated stroma is associated with a worse overall survival [16]. Beyond the interactions with cancer cells and promoting cancer aggressiveness, the presence of stroma limits the delivery of oxygen, resulting in hypoxia [12]. Hypoxia is known to lead to chemotherapy resistance by limiting drug delivery to cells [17] and is also known to promote cancer progression and metastasis through activation of initiating pathways, including hypoxia-inducible factor 1-alpha (HIF-1α) [18, 19]. Overall, this highlights the complexity of PDAC, which in part leads to its difficulty in treatment.

1.1.2 Diagnosis and treatment

Due in part to the retroperitoneal location of the pancreas and lack of visible symptoms with early disease, 57% of PDAC cases are diagnosed at stage IV [20]. Furthermore, 80% of PDAC patients present with unresectable disease at time of diagnosis [21-23]. As such, surgery, which has a 15-25% 5-year survival [24], is not a viable treatment option and lowers the survival to 2% for non-local disease [9]. Risk factors for pancreatic cancer include tobacco smoking [25, 26], pancreatitis [27], and type 2 diabetes [28], which are used to help screen patients for follow-up [12]. Specifically, late onset type 2 diabetes may be an indicator of early pancreatic cancer, and is an active area of research [28].

Gemcitabine was first used to treat metastatic pancreatic cancer in 1997 and there have been few changes to therapy since. When first tested, gemcitabine had an overall survival (OS) of 5.65 months compared to 4.41 months with standard treatment at the time, fluorouracil (5-FU) [29]. Since this discovery, many clinical trials have studied the effect of gemcitabine in

combination with other therapies, but most found no benefit or increased toxicities [30-33]. The combination treatment of gemcitabine and erlotinib had a slight increase in OS (6.24 vs 5.91 months) but also had a higher rate of serious adverse events [31]. Likewise, in 2011 a clinical trial testing FOLFIRINOX, a combination of 5-FU, leucovorin, irinotecan, and oxaliplatin, compared to gemcitabine had a substantial increase in adverse events [33]. However, there was also a considerable difference in overall survival (11.1 vs 6.8 months) [33]. Recently, another impactful trial demonstrated an increased OS with the combination therapy of gemcitabine and nab-paclitaxel (8.7 months compared to 6.7 months with gemcitabine alone) [32]. In Canada today, PDAC patients are either treated with a combination treatment of gemcitabine and nab-paclitaxel or FOLFIRINOX based on health status due to the toxicities that occur with FOLFIRINOX [33].

With the decreasing cost of whole genome and transcriptome sequencing, researchers and clinicians have been able to use these tools to subtype cancers and determine novel targeted therapies. For many cancer types, this strategy has provided clinicians with both new therapies and an enhanced understanding of which therapies may best benefit PDAC patients. While this strategy has enabled researchers to understand the genetic and molecular landscape of the PDAC (described in section 1.1.2 and 1.2.3), many of the current targeted therapies have failed to treat PDAC patients effectively. This is likely due to similar reasons systemic chemotherapy has limited benefit in PDAC: hypoxia and high stromal content [19]. Thus, PDAC is still treated as a singular disease, which further indicates the need for new therapies and predictive markers. Recently, vitamin C has been proposed as a potential treatment for some cancer types and to target *KRAS* mutant colorectal cancers. However, the subtypes of PDAC that may benefit from this therapy remain unclear.

1.1.3 Genetic landscape

Databases such as the Cancer Genome Atlas (TCGA) and the International Cancer Genome Consortium (ICGC) have vastly enhanced our understanding of cancer [6, 34]. The genome and transcriptome data available through these portals have enabled large scale analysis to determine the landscape of PDAC including copy number variations, expression changes, and chromosomal rearrangements. Furthermore, these analyses have been able to determine the major driver events, prognostic subtypes, and pathways to target in PDAC.

The genetic landscape of PDAC largely consists of mutations or alterations in *KRAS*, *TP53*, *SMAD4*, and *CDKN2A* (Figure 1.1) [6, 7, 11, 34]; the major drivers of PDAC [9, 11]. *KRAS* mutations, specifically, are thought to occur early in PDAC development. These oncogenic *KRAS* mutations drive the formation of pancreatic PanIN or IPMN in ductal cells, which then accumulate *TP53*, *SMAD4*, and *CDKN2A* mutations to further promote cancer progression [9-11]. Since *KRAS* is an early driver mutation, 90% of PDAC patients contain *KRAS* mutations [34, 35]. Unfortunately, knowing the driver of this cancer type has not lead to targeted treatments due to the difficult nature of directly inhibiting or targeting *KRAS* [35, 36].

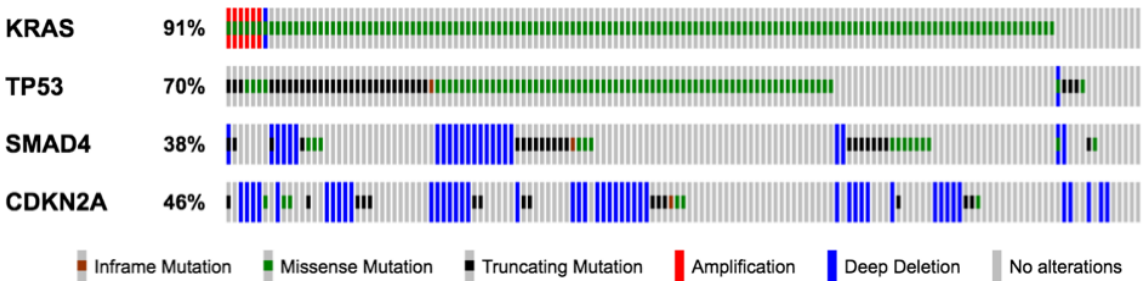

Figure 1.1: Rates of *KRAS*, *TP53*, *SMAD4*, and *CDKN2A* alterations in pancreatic ductal adenocarcinoma (PDAC)
Alteration rates and type in PDAC cases based on data from the Cancer Genome Atlas (TCGA) [34], figure generated in cBioPortal.

KRAS is classified as a GTPase which cleaves the terminal phosphate group on GTP and cycles between active and inactive states when bound to GTP or GDP, respectively [37-39]. The switch between the active and inactive forms of KRAS, as well as other GTPases, is tightly regulated. To activate the GTPase, guanine nucleotide exchange factors (GEFs) exchange GDP for GTP [37-39]. Deactivating the enzyme requires GTPase-activating proteins (GAPs) to cleave the terminal phosphate on GTP, thereby facilitating its conversion to GDP [37-39]. In PDAC, oncogenic KRAS mutations frequently occur in codon 12, which is situated near the GTP binding site. These mutations can also alter the structural conformation of the protein, which results in the reduction of GTP hydrolysis capacity [37, 39]. Together, these mutations serve to promote the sustained active conformation of KRAS, which leads to overstimulation of downstream signalling pathways. Of these, KRAS is involved in three major signalling pathways: the PI3K/AKT/mTOR axis (promoting cell cycle progression and cell migration), the RAF/MEK/ERK axis (promoting cell proliferation and transcription), and the RAL axis (promoting endocytosis and cytokine production) [38]. Thus as cleavage of GTP by KRAS initiates these pathways, the over stimulation due to mutations causes levels of proliferation and survival which contribute to cancer development and progression [38, 39].

To add another layer of complexity in the pursuit of targeted therapies, it is now understood that different *KRAS* mutations can induce different downstream effects [40-42]. For example, studies in lung adenocarcinoma (LUAD) have shown that G12D mutant *KRAS* cancers have increased expression of the PI-3-K/Akt pathway and are not affected by mTOR inhibition [43]. Whereas, in the G12C and G12V mutant *KRAS* cancers the PI-3-K/Akt pathway depends on other growth factors and is subject to mTOR inhibition [43]. Interestingly, rates of *KRAS* mutations differ between cancer types (Figure 1.2). Specifically, based on The Cancer Genome

Atlas (TCGA) data, the most predominant *KRAS* mutation in PDAC are G12D and G12V [34], congruent with other data sources [35]. Whereas, in LUAD the most common *KRAS* mutation is G12C and in colorectal cancer (COAD) the common *KRAS* mutations are G12D and G13D, but at lower prevalence than in PDAC (Figure 1.2) [35]. Furthermore, the subtype which has the worst prognosis differs between cancer type [35, 43, 44]. In LUAD G12V and G12C mutations have a worse overall survival rate compared to the other *KRAS* mutations and *KRAS* WT [43]. However, in PDAC, G12D has the worse prognosis compared to other mutations, adding further complexity to targeting *KRAS* mutant cancers [44]. Interestingly, *KRAS* mutant cancers have been linked to increased dependence on glycolysis and a potential to be more susceptible to reactive oxygen species (ROS) [35, 41, 45, 46]. Other studies have also indicated that the G12D mutation specifically drives glycolytic dependencies and ROS susceptibility [42]. Together these studies indicate potential avenues to treat these aggressive *KRAS* mutant cells through targeting glycolysis and oxidative stress.

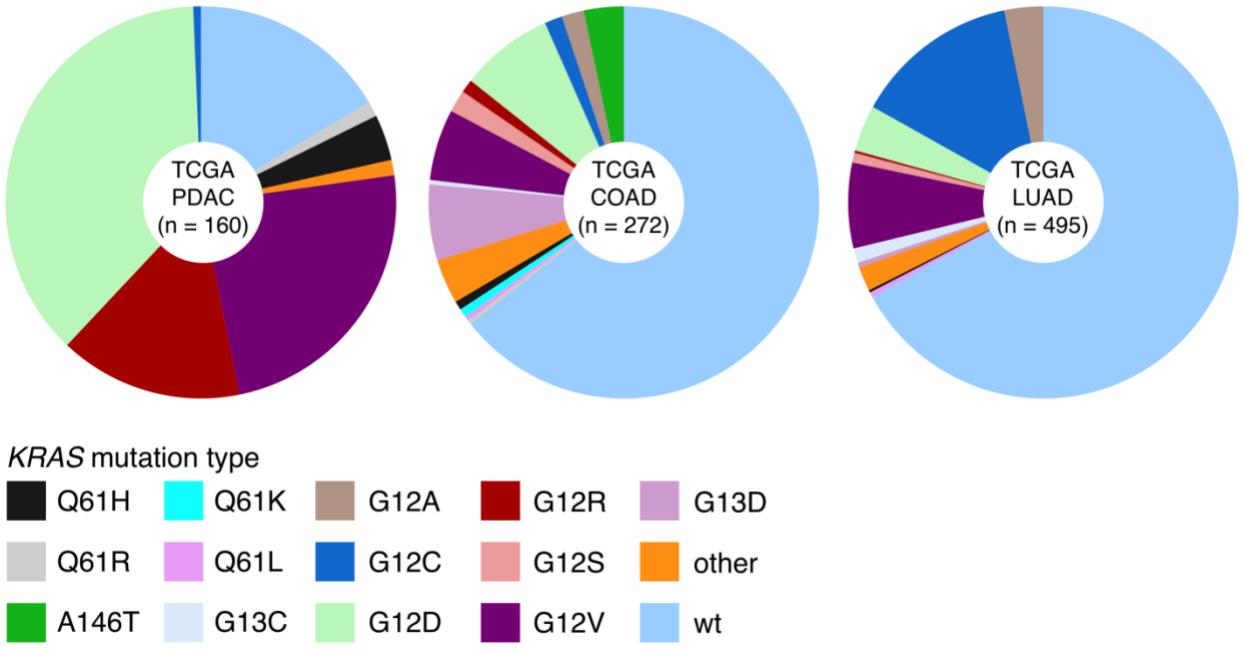

Figure 1.2: Proportion of KRAS mutations in pancreatic ductal adenocarcinoma (PDAC), colorectal cancer (COAD), and lung adenocarcinoma (LUAD)
Graphical representation of the proportion of KRAS mutation types and wild-type (wt) in PDAC, COAD, and LUAD from the Cancer Genome Atlas (TCGA) data [34]. Graph generated by James Topham using R.

Although PDAC has four common mutations that occur in the majority of cases, there is still vast heterogeneity between tumours. Other mutations such as *MLL3*, *TGFBR2*, *SF3B1*, *EPC1*, *ARID1A*, *ARID2*, *MAP2K4*, *ATM*, *NALCN*, *ZIM2*, *MTC4*, occur at rates of less than 10% which increases the difficulty to subtype and treat these cancers [7]. One research group has used rates of mutation events based on whole genome sequencing and have subtyped PDAC into stable, scattered, unstable, and locally rearranged disease [6]. These subtypes are able to depict response to platinum therapy, where the unstable disease subtype, consisting of BRCA1 mutations and DNA damage markers, is an indicator of response [6]. Another study grouped genes and their mutations into pathways and found twelve important cell signalling pathways where alterations occurred in 60-100% of cases [47]. The discovery of these twelve cell

signalling pathways has led to the development of small molecule inhibitors, but currently few have been successful likely due to compensatory mechanisms [48].

1.1.4 Metabolic subtypes

In a search for more tools to aid treatment decisions and patient selection for clinical trials, groups have gone beyond genomic data and investigated the transcriptome to determine subtypes of PDAC (Table 1.1). Initial work done by Collisson et al. [49] distinguished three subtypes (classical, quasi-mesenchymal, and exocrine-like) and associated differences in overall survival among groups. They identified that the quasi-mesenchymal subtype was more sensitive to gemcitabine compared to the classical subtype. In 2015 Moffitt et al. [16] used an algorithm to virtually microdissect the stromal gene expression from the epithelial gene expression. They identified two stromal subtypes (normal and activated stroma) and two epithelial subtypes (classical and basal-like) [16]. They found that the basal-like subtype indicated a worse prognosis but predicted better response to adjuvant chemotherapy [16]. Bailey et al. [50] identified four subtypes associated to histology (squamous, pancreatic progenitor, immunogenic, and aberrantly differentiated endocrine exocrine); the squamous subtype was indicative of a poor prognosis. The prognostic value of Moffitt and Bailey, but not Collisson, have been independently validated [51] and these retrospective analyses show the potential of predictive and prognostic subtypes in PDAC.

Daeman et al. [52] used metabolite profiling in PDAC cell lines and identified three metabolic subtypes (glycolytic, lipogenic, and slow proliferating). They tested a variety of metabolic targeting agents and determined markers which may predict response to these agents [52]. Their study highlighted the utility of metabolic subtypes and the potential of using these subtypes to predict response to treatments that target pathways prevalent to specific subtypes.

While Collisson et al., Moffitt et al. Bailey at al., Daeman et al. and others have provided great insights into PDAC subtypes, more work needs to be done to determine markers that will predict response to new and existing therapies.

Table 1.1: Molecular classifications of pancreatic ductal adenocarcinoma

Classification model	Subtypes	Material used
Collisson	classical, quasi-mesenchymal, exocrine-like	Surgical microdissected epithelium
Bailey	squamous, pancreatic progenitor, immunogenic, aberrantly differentiated endocrine exocrine	Stroma and epithelium
Moffitt	classical, basal-like	Virtual microdissected epithelium
Daeman	glycolytic, lipogenic, slow proliferating	Cell lines

1.2 Vitamin C in cancer

Vitamin C, or ascorbic acid, was first used as a cancer treatment in 1974 by Cameron and Campbell, who treated advanced pan-cancer patients with a combination of oral and intravenous (IV) administered vitamin C and noticed an outcome that was better than would have been expected without intervention [53]. This observation lead to two randomized control trials (RCT) performed at the Mayo clinic [54, 55]. However, neither study was able to demonstrate favourable overall survival in cancer patients receiving vitamin C therapy compared to controls. Campbell et al. [56] completed another retrospective study using 294 cancer patients which received vitamin C therapy during their illness compared to 1532 control cancer patients from the same hospitals which had not received vitamin C therapy. This demonstrated a median overall survival of 343 days in the treated group compared to 180 days in the control group [56].

Unfortunately, his research was ultimately overshadowed by the Mayo clinic's findings due to the small scale and non-randomized trial design, thus work into developing vitamin C as a therapy was abandoned by clinicians.

Pharmacokinetic studies later pointed to the difference in plasma concentrations between IV vitamin C and orally administered vitamin C [57-59]. Specifically, oral doses exceeding 200mg increased excretion, indicating the poor bioavailability of orally administered vitamin C [58, 59]. Alternatively, IV doses of 50g vitamin C were able to reach over 12000μM in plasma [57]. Even when comparing plasma levels using IV vitamin C at the maximum tolerated oral dose of 3g, plasma levels reached 1760μM compared to 206μM with oral vitamin C [57]. These differential plasma levels may explain why Cameron and Campbell were able to see benefit to vitamin C therapy when given as a combination of oral and IV vitamin C [53, 56] while the Mayo clinic found no benefit to therapy in their RCTs using only orally administered vitamin C [54, 55]. Since this discovery, there have been numerous studies into the clinical safety and efficacy of vitamin C therapy and the mechanism of action.

1.2.1 Current clinical research of IV vitamin C toxicity

Phase 1 clinical trials using high doses of vitamin C were aimed at determining the safe doses of injections, plasma level concentrations, and safe regimens in combination with chemotherapy [60-65]. Of the six completed clinical trials (Table 1.2) using high dose IV vitamin C in Canada and the United States, all studies found IV vitamin C to be well tolerated in cancer patients at plasma concentrations upwards of 20mM [60-65]. One group was able to obtain plasma concentrations of 49mM without adverse events [63]. When combined with gemcitabine treatment the only adverse events that were not associated with the gemcitabine monotherapy arm was diarrhea (4/9) and dry mouth (6/9) [60], while other studies showed

maintained or increased quality of life [64]. While none of these phase 1 trials were powered to determine efficacy, researchers noted an increased overall survival in their small cohorts of 13 months [60] or 15.1 months [61]. Another group performed CT scans before and after gemcitabine, erlotinib, and vitamin C combination treatment revealing that 8 of 9 cases had decreased tumour size, which is atypical for gemcitabine and erlotinib treatment in PDAC [62]. Together, these data indicate that high dose IV vitamin C is safe and suggests that there is a clinical benefit, but larger studies are necessary. In response to these promising phase 1 trials, there are ongoing phase 2 clinical trials to determine the efficacy of vitamin C therapy in cancer (Table 1.3). However, to optimally determine the role of vitamin C in pancreatic cancer, there is a need to understand which subsets of PDAC patients will respond to this therapy. While knowing the mechanisms of action (described in section 1.2.2) are beneficial to the overall understanding of the therapy, more biomarker studies are required.

Table 1.2: Completed clinical trials of IV vitamin C in Canada and the United States (Clinicaltrials.gov, December 28, 2018)

NTC ID	Condition	Treatment	Study Phase	Outcome measures	PMID
NCT01833351	Healthy normal, cancer patients	Vitamin C only	Phase 1	*Primary Outcome:* Maximum tolerated dose *Secondary Outcome:* Biochemical and physiological effects of intravenous ascorbic	Not Available
NCT00441207	Solid tumours	Vitamin C only	Phase 1	*Primary Outcome*: Adverse event frequency categorization as a measure of safety and tolerability *Secondary Outcome:* Vitamin C accumulation with repeated daily therapy by measuring peak and nadir levels, quality of life	23670640
NCT01049880	Pancreatic cancer	Vitamin C + gemcitabine	Phase 1	*Primary Outcome:* Blood cell counts (neutropenia, thrombocytopenia) and serum chemistries (liver function tests, creatinine) *Secondary Outcome:* Plasma ascorbate level (targeted to 350 to 400 mg/dL), overall survival	23381814
NCT01364805	Pancreatic cancer	Vitamin C + gemcitabine	Phase 1	*Primary Outcome:* Safety of combined gemcitabine chemotherapy with IV ascorbate. *Secondary Outcome:* Pharmacokinetic and pharmacodynamic interactions of combination therapy	29215048
NCT00954525	Pancreatic cancer	Vitamin C + gemcitabine + erlotinib	Phase 1	*Primary Outcome:* Safety, assessed by toxicity (graded by NCI CTC), urinalysis, ECG, basic metabolic panel, CBC, and osmolality. *Secondary Outcome:* Progression-free survival	22272248
NCT01050621	Advanced cancer	Vitamin C + standard of care	Phase1/2	*Primary Outcome:* Adverse event frequency categorization as a measure of safety and tolerability *Secondary Outcome:* Disease arrest or response, quality of life assessment, measure the effect of chemotherapy on pharmacokinetics of IV ascorbic acid	25848948

Table 1.3: Ongoing clinical trials of IV vitamin C in Canada and the United States (Clinicaltrials.gov, December 28, 2018)

NTC ID	Condition	Additional Treatment	Study Phase	Outcome measures
NCT03508726	Soft tissue sarcoma	Vitamin C only	Phase 1B/2	*Primary Outcome:* Adverse event frequency and categorization *Secondary Outcome*: Pathological complete response rates, time to disease progression, overall response rate, labile iron, evaluate diffusion weighted imaging sequences
NCT03410030	Metastatic pancreatic cancer	Vitamin C + nab-paclitaxel + cisplatin + gemcitabine	Phase 1B/2	*Primary Outcome:* Phase IB: maximum tolerated dose Phase II: Disease control rate *Secondary Outcome:* Overall survival, progression free survival, changes in patient's self-reported quality of life, changes in patient's self-reported pain levels
NCT03146962	Colorectal, pancreatic, lung cancers	Vitamin C only	Phase 2	*Primary Outcome:* Pathologic response based on tumor regression grading in cohort A patients. 3-month disease control rate in cohort B patients. *Secondary Outcome:* Progression-free survival in cohort B, objective response rate in cohort B, assessment of pharmacokinetics of high dose vitamin C plasma levels concentrations, adverse event frequency categorization
NCT02344355	Glioblastoma	Vitamin C + radiation + temozolomide	Phase 2	*Primary Outcome:* Overall Survival *Secondary Outcome:* Adverse event frequency categorization
NCT02420314	Lung cancer	Vitamin C + nab-paclitaxel + carboplatin	Phase 2	*Primary Outcome:* Tumor response *Secondary Outcome:* Progression free survival, overall survival, adverse event frequency categorization
NCT02905591	Lung cancer	Vitamin C + radiation + nab-paclitaxel+ carboplatin	Phase 2	*Primary Outcome:* Progression rate *Secondary Outcome:* Progression free survival, overall survival, adverse event frequency categorization

NCT02905578	Pancreatic cancer	Vitamin C + gemcitabine + nab-paclitaxel	Phase 2	*Primary Outcome:* Overall survival *Secondary Outcome:* Progression free survival, adverse event frequency categorization
NCT03541486	Pancreatic cancer	Vitamin C + radiation + gemcitabine	Phase 2	*Primary Outcome:* Overall survival *Secondary Outcome*: Objective response rate, progression free survival
NCT03468075	Sarcoma	Vitamin C + gemcitabine	Phase 2	*Primary Outcome:* Tumor response *Secondary Outcome*: Progression free survival, overall survival, adverse event frequency categorization

1.2.2 Mechanisms of vitamin C activity in cancer

Studies have identified that physiological doses of vitamin C can aid in cancer treatment by acting as a co-factor for both ten-eleven translocation (TET) dioxygenases and HIF1-α hydroxylases, which can aid in reducing the aggressiveness of cancer [66-72]. However, pharmacological doses can cause oxidative stress through the accumulation of hydrogen peroxide (H_2O_2), leading to cancer cell death [73-82]. The current knowledge of these mechanisms of vitamin C activity in cancer are described in the following two sections.

1.2.2.1 Physiological doses of vitamin C in cancer

Cancer patients have been known to have deficiencies in anti-oxidants, including vitamin C [83, 84]. Since vitamin C is a co-factor for many regulatory enzymes involved in cancer progression, researchers hypothesized that the lack of vitamin C in cancer patients may lead to cancer development and progression [83, 84]. For instance, vitamin C acts, as mentioned above, as a co-factor for TET dioxygenases and supplementation of vitamin C increases the function of TET dioxygenases [66-68]. This leads to DNA demethylation resulting in the reactivation of tumour suppressor genes in lymphoma and leukemia [66-68].

Similar to the co-factor interaction between vitamin C and TET, physiological levels of vitamin C have been suggested to suppress HIF1-α under both normoxia and hypoxia [69-71], a common event in PDAC tumours [19, 85]. This occurs since vitamin C is needed for the activity of HIF1-α hydroxylases which in turn inactivates HIF1-α [71]. HIF1-α is known to upregulate genes involved in glycolysis and glucose transport, promoting cancer progression [86]. Thus, inactivating HIF1-α in cancer patients is an active research topic. In colorectal cancer patients, there is an inverse association between vitamin C in the tumour and activation of HIF1-α, which supports the notion that vitamin C may inactivate HIF1-α [72]. It has been further suggested, that

vitamin C deficiency seen in cancer patients may drive the HIF1-α dependent phenotype and result in a lower disease-free survival [72]. Together these studies suggest that physiological levels of vitamin C may be important in the regulation of HIF1-α and TET, and subsequently physiological vitamin C supplementation may have the potential to reduce the aggressiveness of cancer cells. However, these mechanisms are unable to describe the direct cytotoxicity that occurs after vitamin C administration.

1.2.2.2 Pharmacological doses of vitamin C causing oxidative stress and cytotoxicity in cancer

Pharmacological doses (>100μM) of vitamin C could be used as treatment to kill cancer cells through the accumulation of H_2O_2, which leads to oxidative stress and ultimately cell death [73-82]. Interestingly, vitamin C increases levels of H_2O_2 only at plasma doses achieved by IV administration, compared to oral vitamin C [74, 80]. In fact, one report described that administration of 7.5mM vitamin C IV increased H_2O_2 to 20μM from undetectable levels in mice [74]. Furthermore, adding H_2O_2 at comparable levels to that produced by pharmacological vitamin C caused similar levels of toxicity compared to vitamin C alone [74, 77] and adding H_2O_2 scavengers in combination with *in vitro* vitamin C completely eliminated toxicity [73-79]. Another group proposed that in colorectal cancer cells dehydroascorbic acid (DHA) leads to cell death [87]. Mechanistically, H_2O_2 [88-90] and intracellular DHA [91, 92] both decrease levels of glutathione (GSH), which can sensitize cells to oxidative stress [76, 93-97]. However, while DHA increases levels of intracellular vitamin C to the same extent as vitamin C, DHA is unable to cause cytotoxicity [74, 82], indicating that DHA is not sufficient on its own to deplete GSH and cause oxidative stress. Therefore, despite these promising results, untested H_2O_2 levels likely account for the toxicity observed in this study.

Vitamin C causes toxicity in cancer cells at doses that do not harm normal cells [76, 79, 81]. One reason for this selective toxicity in cancer cells may be that the rate of H_2O_2 removal is higher in normal cells compared to cancer cells [81]. Others have related this selective toxicity to increased sensitivity to oxidative stress due to metabolic changes caused by glycolytic dependence [75], which often occurs in cancerous cells [98]. Yun et al. [87] recently proposed that vitamin C caused selective toxicity in *KRAS* and *BRAF* mutant colorectal cells. Together these results highlight the potential of pharmacological doses of vitamin C as a therapy to selectively target cancer cells, but leads to questions of whether all cancer cells will be targeted.

1.3 Rationale, Hypothesis and objectives

Pancreatic ductal adenocarcinoma is difficult to treat [1, 3], with most patients presenting with metastatic disease [21-23], which quickly becomes resistant to chemotherapy [19]. Unlike other cancer types where there have been advancements in targeted therapies, PDAC consists of a majority of *KRAS* mutant tumours [34, 35], which are notoriously difficult to target and exacerbated by absence of *KRAS*- molecular targeting therapeutics [35, 36]. Furthermore, these *KRAS* mutations often cause alterations in glycolysis and oxidative stress pathways, and these pathways have been suggested as targets for these cancers [35, 43]. Through mechanistic studies, IV vitamin C treatment has been suggested to alter glycolysis and cause an increase in oxidative stress, leading to cell death [75]. This suggests that vitamin C therapy may be beneficial for *KRAS* mutant PDAC. Moreover, Yun et al. [87] recently connected vitamin C toxicity to *KRAS* mutant colorectal cancer, further demonstrating the need to study vitamin C toxicity in relation to *KRAS* mutations in PDAC. Therefore, we hypothesized that:

The presence of KRAS *mutations indicates sensitivity to vitamin C therapy in PDAC.*

To answer this hypothesis, we set out the following objectives.

Objective 1: Determine the association of distinct *KRAS* mutations with vitamin C cytotoxicity

Aim 1.1: Determine vitamin C toxicity in *KRAS* mutant and wildtype cell lines

Aim 1.2: Create isogenic *KRAS* mutant PDAC cell lines and investigate the effect of induced *KRAS* mutations in vitamin C toxicity in PDAC cells

Objective 2: Investigate the selective toxicity of vitamin C with cellular processes associated to cell metabolism

Aim 2.1: Determine the potential of glutathione as a marker of vitamin C sensitivity

Aim 2.2: Investigate the relationship between vitamin C cytotoxicity and glycolysis

Objective 3: Determine if vitamin C is cytotoxic in patient-derived models with unique mutational signatures

Chapter 2: Materials and methods

2.1 Cell lines and Culture

Human cell lines MIA Paca-2, BxPC-3, HPAF-II, Panc-1, Hs766T, Capan-2, HEK 293T, and HPNE were gratefully received from Dr. Marcel Bally. Paca41.7 was created from patient-derived xenograft tissue using a modified protocol for pancreatic cell isolation modified by Dr. Janel Kopp and Dr. Joanna Karasinska based on published protocols [99, 100]. J38 #421 mouse epithelial cell line (MEC) was gratefully received from Dr. Janel Kopp; created and cultured based on published protocols [99, 100]. MIA Paca-2, Panc-1, Hs766T, Capan-2, and HEK cells were cultured in DMEM (Thermo Fisher, 11995073) supplemented with 10% fetal bovine serum (FBS) (Thermo Fisher, 12483-020). BxPC-3 cells were cultured in RPMI (Thermo Fisher, 11875119) with 10% FBS and HPAF-II cells were cultured in EMEM (ATCC, 30-2003) with 10% FBS. HPNE cells were cultured in 75% DMEM and 25% M3:Base (INCELL, M300F) supplemented with 10 ng/mL human recombinant EGF, 750 ng/mL puromycin (Thermo Fisher, A1113803) and 5% PBS. D- Glucose (Sigma, G8270) was prepared as a 333mg/ml stock in sterile water and sterile filtered.

Cells were grown at 37°C in 5% CO_2. Experiments were conducted in DMEM media (Gibco, 11966-025), 10% FBS, supplemented with either 2mM or 20mM glucose. Gemcitabine (EliLilly Pharmacy, V-7502), was diluted to a final concentration of 0-1mM. Sodium Ascorbate (Sigma, a7631) was dissolved into media prior to experiments to a final concentration of 0-20mM. L- glutathione (Sigma, G6013) was dissolved into media prior to experiments to a final concentration of 5mM.

2.2 Mutant *KRAS* isogenic line creation

2.2.1 G12V

P20-KRAS-G12V (Addgene, 44012, with cDNA insert for *KRAS* G12V) plasmid, P20-GFP plasmid (Addgene, 44012), psPAX2 lentiviral packaging plasmid (Addgene, 12260), and pmDG VSV-G envelope plasmid (Addgene, 12259) were graciously donated by Dr. William Lockwood (BCCRC) [101]. Lentivirus particles containing P20-KRAS-G12V or P20-GFP were generated by transfecting 3.42µg P20-KRAS-G12V or P20-GFP plasmid with 1.71µg psPAX2 and 0.86µg pmDG plasmids and 12µl of Lipofectamine 2000 (Thermo Fisher, 11668027) with 700,000 HEK 293T cells in a CL2+ facility. Media containing lentivirus was filtered and used immediately.

Hs766T and BxPC-3 cells were seeded in 6 well plates at 200,000 cells per well in 3ml DMEM (Gibco) media. After 24 hours, cells were taken to the CL2+ facility. Media was removed and replaced with media from one well of HEK 293T plate producing P20-KRAS-G12V or P20-GFP lentivirus particles supplemented with 8µg/ml polybrene (Sigma, H9268). Each condition was applied to two plate wells in duplicate. Plates containing lentivirus virus were spun at 1200g for 1 hour at 37°C, and subsequently incubated for 24 hours at 37°C and 5% CO_2. Virus was removed and fresh virus was added to each well and spun at 1200g for 1 hour at 37°C. After an additional 24-hour incubation at 37°C and 5% CO_2, cells were washed and removed from the CL2+ facility. Selection of transfected cells was performed using geneticin (Gibco, 10131). Geneticin concentration was optimized on parental BxPC-3 and Hs766T cells using IncuCyte ZOOM (ESSEN Bioscience) phase contrast analysis (Figure 2.1a). Media containing 1000µg/ml Geneticin was added to each well in addition to non-transfected cells. Cells were monitored for cell death and cells remained in antibiotic containing media until all

control cells were dead (4 days). After selection, transfected cells were cultured in DMEM containing 10% FBS.

2.2.2 G12D

KRAS G12D, *KRAS* WT, and non-targeting control (NTC) lentivirus particles were ordered from GeneCopoeia (Table 2.1). Each lentivirus transfer vector (pEZ-Lv201) contained VSV-G protein, GFP reporter, puromycin resistance gene, and CMV promotor driving expression of the inserted gene. Briefly, lentivirus particles were generated by GeneCopoeia by co-transfection of the transfer vector into HEK 293a cells (GeneCopoeia, CLv-PK-01) with Lenti-Pac HIV packaging mix (GeneCopoeia, HPK-LvTR-20). Lentivirus was purified and validated by full length sequencing, restriction enzyme digest, and PCR validation prior to receiving.

Table 2.1 Purified lentivirus particles from GeneCopoeia

Catalog Number	Given Name	Insert	Titer
LPP-NEG-Lv201-025-C	NTC	Non-Targeting control	$2.8x10^8$ TU/ml
LPP-T0178-Lv201-050	KRAS WT	KRAS (NM_004985.4)	$1.73x10^8$ TU/ml
LPP-CS-T0178-Lv201-01-050	KRAS G12D	KRAS (NM_004985.4) with G12D/G35A mutation	$2.11x10^8$ TU/ml

Hs766T and BxPC-3 cells were seeded in 6 well plates at 200,000 cells per well in 3ml DMEM media. After 24 hours, cells were taken to the CL2+ facility. Media was removed and replaced with *KRAS* WT, *KRAS* G12D, or *KRAS* NTC lentivirus particles at 5 multiplicity of infection (MOI) with 8µg/ml polybrene (Sigma, H9268). Each condition was applied to two separate plate wells. Plates were spun at 1200g for 1 hour at 37°C. Virus was removed and washed 24 hours after and removed from the CL3 facility. Media containing 2µg/ml puromycin was added to the transfected and non-transfected cells. Prior to selection, optimal puromycin

concentration was determined on parental BxPC-3 and Hs766T cells using IncuCyte ZOOM phase contrast analysis (Figure 2.1b). Cells were monitored for cell death and remained in puromycin containing media until the non-transfected controls were all dead (4 days). Going forward, cells were then maintained in DMEM containing 10% FBS.

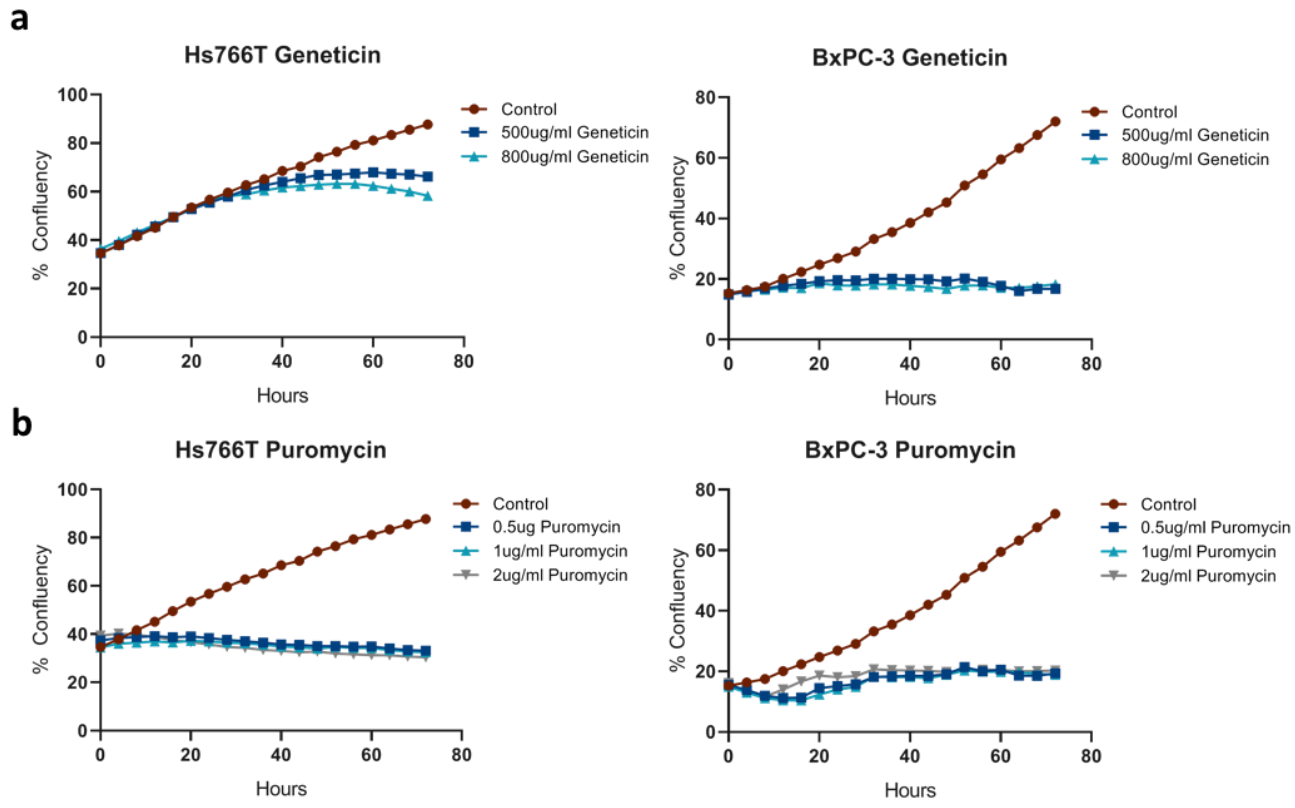

Figure 2.1: Antibiotic growth inhibition in Hs766T and BxPC-3
Cells were treated with geneticin **(a)**, puromycin **(b)** or control for 72 hours. Images were taken every 4 hours by IncuCyte ZOOM and confluency was determined using phase contrast analysis

2.3 Organoid lines and Culture

Organoids were derived and expanded as described previously [102], with minor modifications. Organoids were created from either xenograft patient-derived tissue to create xenograft patient-derived organoids (xPDOs) or metastatic biopsy tissue to create metastatic patient-derived organoids (mPDOs). Organoid growth media was made using advanced DMEM (Thermo Fisher, 12634010) containing 1% GlutaMax (Gibco, 35050061), 2% vitamin B27

(Thermo Fisher, 17504044), 0.5% insulin (Thermo Fisher, 12585014), 280μM vitamin C (Sigma, A7631), 8μM hydrocortisone (Sigma, H0888), 0.1μM All Trans Retinoic Acid (Stemcell Tech, 72262), 0.05% human EGF (Cedarlane, AF-100-15), and 6nM human recombinant bFGF (Stemcell Tech., 78003). Briefly, cells were cultured in organoid growth media supplemented with 5% matrigel (VWR, 354230) and 10μm ROCK inhibitor (Tocris, 1254) on a layer of matrigel. Cells were grown at 37°C in 5% CO_2.

2.4 Cell Proliferation assays

Cells were seeded in a 96 well plate (Greiner Bio-one, 655090) at 5000 cells/well in either 20mM D-glucose or 2mM D-glucose media and placed in an IncuCyte ZOOM. Images were taken every 1-4 hours for 5 days and images were analyzed using phase contrast to determine well confluency at each time point. Data was exported and doubling time was calculated using the following formula:

$$\frac{incubation\ time * \ln 2}{\ln \frac{cell\ confluncy_{end}}{cell\ confluency_{start}}}$$

2.5 Cell viability assays

Hoechst 33342 and ethidium homodimer were used to determine cell viability. Hoechst 33342 binds to double stranded DNA and emits blue fluorescence, and permanently stains all cells. Ethidium homodimer-1 is cell-impermeant and binds to nucleic acid producing a red fluorescence. Due to its impermeability, this stain only binds to the nucleic acid of dead cells. The IN Cell Analyzer 2200 (GE Healthcare) in combination with the Workstation 3.7.3 software were then used to take and analyze images under both blue and red channels to count both live and dead cells. Thus, this system is able to determine both changes in viability as well as proliferation.

To assess cell viability and proliferation, cells were seeded in a 96-well plate (Greiner Bio-one, 655090) at 5000 cells/well. After 24 hours, cells were exposed to controls or drugs at various concentrations (described in section 2.1). Drugs were serial diluted to achieve desired concentrations. In each experiment, the volume of vehicle control used was equal to the highest volume used with the drug. After desired treatment time, ranging from 24-72 hours, plates were incubated with 130µM or 260µM Hoechst 33342 (Invitrogen, H3570) and 1µM or 2.5µM ethidium homodimer-1 (Invitrogen, E1169) for 15 or 60 minutes, for cells and organoids respectively, to distinguish between viable and dead cells. Plates were then imaged using the IN Cell Analyzer 2200. Images were analyzed with the Workstation 3.7.3 software and cell viability was calculated, normalized to the untreated control, and graphed using GraphPad Prism8.

2.6 Flow cytometry

Flow cytometry was also used to determine cell viability. Cells were trypsinized (0.25%, Gibco, 25200), washed in phosphate- buffered saline (PBS) (Thermo Fisher, 10010-049) and re-suspended in PBS containing 30nM SYTOX Green (Thermo Fisher, S7020) for 20 minutes. Single-cell suspensions were analyzed using BS CellQuest Pro5.2.1 on a Becton Dickinson FACSCalibur.

2.7 Western Blots

Cells were either trypsinized (0.25%, Gibco, 25200) or scrapped and then washed with PBS (Thermo Fisher, 10010-049) to create cell pellets. Cell pellets were lysed in RIPA buffer (Thermo Fisher, 89900), Protease inhibitor cocktail (Roche, 05892970001), and phosphatase inhibitor cocktail (Roche, 4906845001) for 1 hour on ice. Supernatant was collected following centrifugation at 14000 RPM for 15 minutes at 4°C. Protein was quantified using the Pierce bicinchoninic acid protein assay (Thermo Fisher, 23235) according to manufacturer instructions. To prepare each sample, 20µg of protein was treated with LDS sample buffer (Invitrogen,

NP0007) and β-mercaptoethanol (Sigma, M6250) and heated 15 mins at 70°C. Samples were run on a NuPAGE 4-12% Bis-Tris protein gel (Invitrogen, NP0322) using NuPAGE MES SDS Running buffer (Novex, NP0060). Gels were then transferred to nitrocellulose membrane (BIO RAD, 1704159) using BIORAD Trans-Blot Turbo Transfer System and blocked in 5% skim milk in TBST (0.24% TRIZMA base (Sigma), 0.8% Sodium Chloride and 0.1% Tween20 (Sigma).

Membranes were probed with antibodies against either KRAS G12V (1:1000; Cell Signalling, 14429), KRAS G12D (1:1000; Cell Signalling, 14412), β-actin (1:50000; Sigma, A1978) in 5% skim milk overnight at 4°C. Membranes were then washed and probed in 5% skim milk with goat anti-rabbit IgG-HRP antibody (1:5000, KRAS G12D and KRAS G12V; Promega, W4011) or anti-mouse IgG-HRP antibody (1:10000, β-actin; Promega, W4028) for 1 hour at room temperature. Detection of chemi-luminescence was obtained after application of ECL detection reagents (GE Healthcare, RPN2209) and exposure to ECL Hyperfilm (GE Healthcare, 28906839).

2.8 Glycolytic stress tests

Glycolytic Stress tests (Aligent, 103020) were performed to determine cellular glycolysis using an XFe96 Analyzer (Seahorse Bioscience) according to manufacturer's instruction with optimized drug, cell, and substrate concentrations. Briefly, MIA Paca2 and BxPC-3 cells were seeded in Seahorse XFe96 well plates at 1.5 x 10^4 cells in XF base assay medium. Three sequential measurements of the extracellular acidification rate (ECAR) were taken prior to experiment (basal conditions). Cells were then exposed to 3mM vitamin C or control for 2 hours and 12 measurements were taken. Glycolytic stress test was then performed and three sequential measurements were obtained following each drug addition of the kit (glucose, oligomycin, and 2-DG). The addition of glucose allows detection of glycolysis rates, while oligomycin inhibits

ATP synthase which allows the detection of the glycolytic capacity of each condition. Finally, 2-DG, a competitive inhibitor of glucose, causes ECAR to reduce back to basal levels, enabling the detection of glycolytic reserve.

Data were normalized using confluency determined by IncuCyte ZOOM analysis. Replicates were averaged to give mean +/- SEM.

2.9 GSH/GSSG ratio analysis

To assess oxidative stress, total glutathione (GSH) and GSH to oxidized glutathione (GSSG) ratios were determined under basal conditions. GSH to GSSG ratios were determined using Promega GSH/GSSG-Glo Assay (Promega, V6611) according to manufacturer's instructions. Briefly, cells were seeded in triplicates at 5000 cells per well into a 96 well plate (Greiner Bio-one, 655098) and incubated at 37°C. Following 24 hours, total cell confluency was determined using IncuCyte Zoom. Growth media was removed and cells were incubated with sterile water or 3mM vitamin C for 2 hours. Water or vitamin C was removed and 50µL of Total Glutathione Lysis Reagent or Oxidized Lysis Reagent were added to each well and incubated shaking at room temperature for 5 minutes. 50µL of Luciferin Generation Reagent was then added to each well and shaken for 1 minute prior to 30-minute incubation at room temperature. Following incubation, 100µL of Luciferin Detection Reagent was added to each well, shaken for 1 minute, and incubated at room temperature for 15 minutes. Luminescence was measured using FLUOstar OPTIMA1.2 (BMG). Wells were normalized to cell density and triplicates were averaged within each replicate. GSH/GSSG ratio was determined using the following calculation:

$$\frac{Net\ total\ GSH\ RLU - Net\ GSSG\ RLU}{\frac{Net\ GSSG\ RLU}{2}}$$

Spearman's correlations were used to determine correlation between basal glutathione levels or change in glutathione levels compared to cell viability to vitamin C.

2.10 Data interpretation and statistical analysis

All data was visualized and analyzed on GraphPad Prism (version 8.0.0, San Diego, California, USA)

Chapter 3: Results

3.1 High dose vitamin C toxicity in PDAC and non-malignant cell lines

To understand the landscape of vitamin C toxicity in PDAC cell lines, seven PDAC cell lines (Table 3.1) and three non-malignant cell lines were used. Prior to IN Cell analysis, cells were stained with hoechst 33342, a nucleic acid stain that is permeable to cell membranes and ethidium homodimer-1, a stain impermeable to cell membranes that specifically stains dead cells. This method was chosen for viability analysis over other common methods, such as the MTT assay, because vitamin C is known to alter redox pathways and can reduce MTT (3-[4,5-dimethylthiazol-2-yl]-2,5-diphenyltetrazolium bromide) to formazan, leading to potentially confounding results [103]. Therefore, IN Cell analysis was chosen since it can determine viability directly, rather than relying on detecting changes in metabolic output.

Table 3.1 PDAC cell line characteristics

Cell line	*KRAS*	*TP53*	Origin
MIA Paca2	G12C	R248W	Primary tumour
Panc-1	G12D	R273H	Primary tumour
Paca41.7	G12V	ND*	Pancreas Centre BC derived PDAC cell line from patient-derived xenograft tissue
Capan-2	G12V	WT	Primary tumour
BxPC-3	WT	Y2220C	Primary tumour
Hs766T	WT	WT	Lymph node metastasis
HPAF-II	G12D	P151S	Ascites

*ND= not determined

The viability of PDAC cells was tested using vitamin C doses between 0 and 2.5mM (Figure 3.1a) and resulted in variable sensitivity. Toxicity at doses beyond 2.5mM were indeterminable using IN Cell due to crystal formation interfering with analysis (Figure 3.1b-c). Therefore, to determine vitamin C toxicity at doses higher than 2.5mM, flow cytometry was

performed on selected cell lines. This analysis of vitamin C treatment resulted in cytotoxicity at doses larger than 2mM in cell lines that were unresponsive at the lower doses (Figure 3.1d). However, we also observed death between 2mM and 3mM in the non-malignant control (HPNE), indicating that the therapeutic window for cell lines is between 0 and 3mM for these experimental conditions. To further determine if vitamin C is toxic to non-malignant cells, we tested three non-malignant cells using IN Cell analysis. The non-malignant cells began to die at doses of 1.5mM and greater ($p<0.0001$, 1.5mM compared to control for HPNE and HEK) (Figure 3.1e). Thus, 1.5mM, a dose consistent with toxicity in another study in pancreatic cancer [90], was chosen for comparisons of toxicity among PDAC lines. To understand whether oncogenic *KRAS* mutant cells were more susceptible to vitamin C toxicity, as previously described in colorectal cancer [87], we segregated viability based on *KRAS* mutation status (Figure 3.1f). *KRAS* WT cells were not sensitive to vitamin C whereas the majority of *KRAS* mutant cells were sensitive, in line with results in colorectal cancer [87]. Together this highlighted the need to further investigate the role of oncogenic *KRAS* as a marker of vulnerability in PDAC.

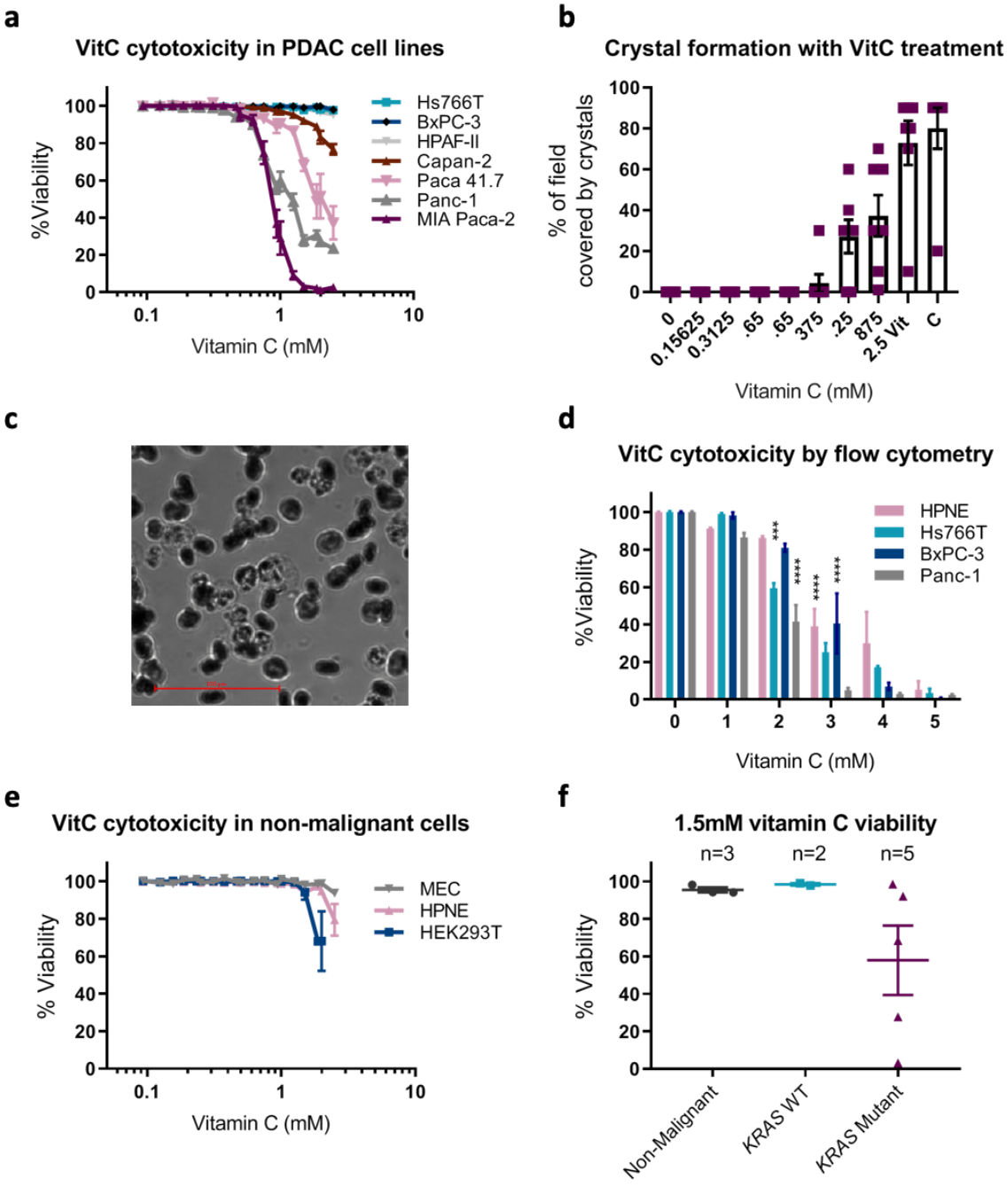

Figure 3.1: Vitamin C differential toxicity in PDAC cell lines
(**a**) Viability curves of PDAC cell lines after 24-hour treatment with vitamin C (VitC) (0-2.5mM) using IN Cell analysis. (**b**) Bar graph of estimated crystal formation after exposure to vitamin C (1-5mM) (**c**) Brightfield image of MIA Paca-2 cells treated with 2.5mM vitamin C (**d**)Viability bar graphs of PDAC and non-malignant HPNE cells treated with vitamin C (0-5mM) for 72 hours and stained with SYTOX Green to test for viability by flow cytometry. ***p<0.001, ****p<0.0001, compared to respective controls, two-way ANOVA Tukey's multiple comparisons test (**e**) Viability curves of non-malignant cell lines treated with vitamin C (0-2.5mM) for 24 hours tested with IN Cell analysis. ****p<0.0001, 1.5mM compared to control for HPNE and HEK, two-way ANOVA Tukey's multiple comparisons test (**f**) Plot of single dose (1.5mM) viability from data used for Figure3.1**a** segregated based on KRAS mutation.

3.2 High dose vitamin C toxicity in isogenic *KRAS* mutant cell lines

3.2.1 Generation of *KRAS* G12V and *KRAS* G12D mutant cell line models

While the initial screen of PDAC cell lines suggests that *KRAS* mutations may play a role in vitamin C vulnerability, we sought to manipulate our non-sensitive *KRAS* WT PDAC cell lines to express oncogenic *KRAS* with the aim of altering their sensitivity to vitamin C. As mentioned previously, *KRAS* G12D and G12V mutations are the two most common *KRAS* mutations in PDAC cells [34, 35], and thus were chosen for further *in vitro* experiments. The analysis of these specific mutations provided the opportunity to test multiple *KRAS* mutations that are present in the majority of patients with PDAC. To establish the appropriate gene-editing method, CRISPR point mutation gene transfection was first considered. Targeting CRISPR plasmids and donor plasmids were created with guidance from Dr. Francis Lynn. However, initial transfection experiments using these plasmids failed to yield viable cells using different transfection conditions, thus lentiviral transfection was explored. Lentiviral transfection provides an advantage over zinc finger nucleases and transcription activator-like effector nucleases as it allows for the accurate and efficient cell manipulation qualities. Therefore, expression of *KRAS* G12V and *KRAS* G12D mutant protein through lentivirus transfection was established in our two WT *KRAS* PDAC cell lines, Hs766T and BxPC-3. The generation of these two model systems with respective controls and their response to vitamin C treatment is described below (section 3.2.1.1, section 3.2.1.2, and section 3.2.2).

3.2.1.1 Transfection of Hs766T and BxPC-3 with G12V mutant *KRAS* lentiviral vectors

To create *KRAS* G12V expressing PDAC cell lines from our two WT *KRAS* lines, a lentivirus transfection technique was used with plasmids previously constructed by Dr. William Lockwood [101]. Integration of the open reading frame (ORF) and subsequent antibiotic selection (described in section 2.2.1) allowed the generation of cell lines containing inducible

KRAS G12V expression that could be used in following experiments (Table 3.2). This system exploits a doxycycline (Dox) inducible mechanism to "turn on" expression of the *KRAS* mutant protein or Green fluorescent protein (GFP) control (Figure 3.2). After isolation of cells containing the ORF, cells were exposed to Dox to "turn-on" the expression of the ORF. To validate expression of the ORFs, fluorescent microscopy and western blots were performed to detect cells expressing GFP and *KRAS* G12V respectively. As expected, GFP expression was observed in our Hs766T GFP-containing cells (HSdGFP) and BxPC-3 GFP-containing cells (BXdGFP) only after the addition of Dox (Figure 3.3a). Furthermore, increasing Dox concentrations led to a dose dependant increase of the expression of KRAS G12V in HSdG12V and BXdG12V (Figure 3.3b). Together, these results confirm the successful transfection of *KRAS* G12V into Hs766T and BxPC-3, as well as successful production of *KRAS* mutant protein under Dox activation.

Table 3.2: Summary of isogenic *KRAS* G12V model cell lines

Cell line name	Parental cell	ORF
BXdG12V	BxPC-3	Dox inducible *KRAS* G12V
BX dGFP	BxPC-3	Dox inducible GFP
HSdG12V	Hs766T	Dox inducible *KRAS* G12V
HSdGFP	Hs766T	Dox inducible GFP

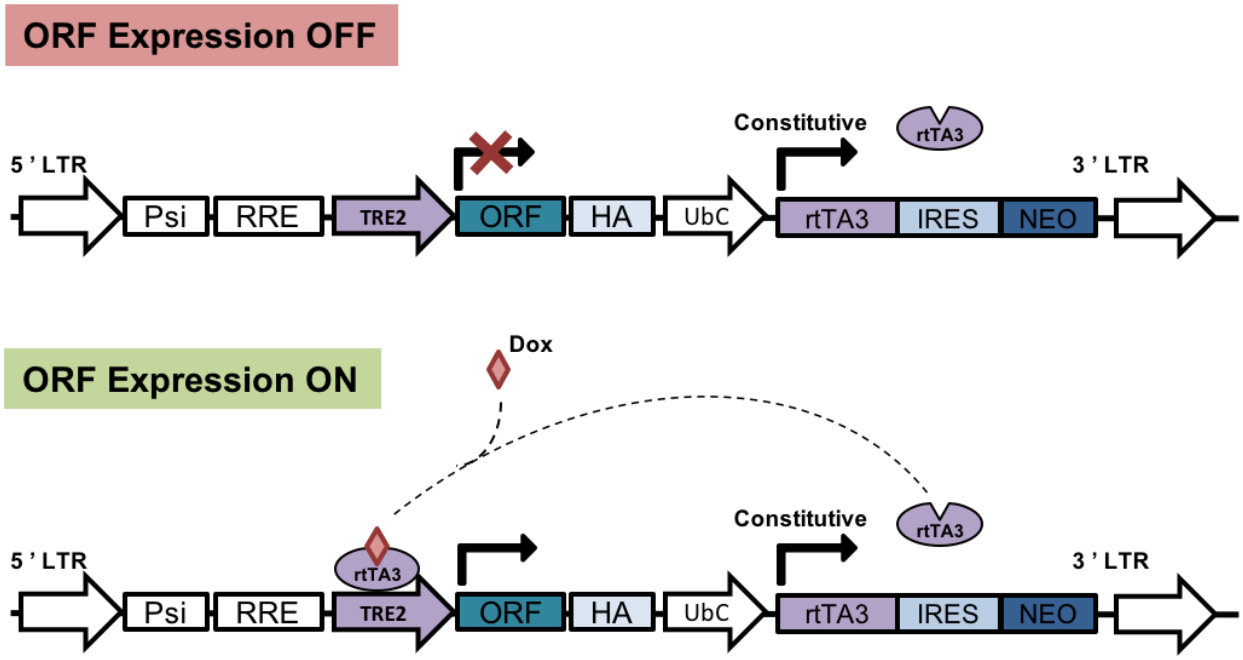

Figure 3.2: Diagram of TET-ON system for *KRAS* G12V model system
Doxycycline (Dox) is used to induce expression of the open reading frame (ORF) containing either *KRAS* G12D or *GFP*. Tetracycline transactivator (rTA3) is constitutively expressed, however on its own it is unable to bind to the tetracycline response element (TRE2) indicating expression of the ORF is "OFF". When rTA3 is bound to tetracycline, or a derivative such as Dox, it can bind to TRE2 to turn the ORF expression "ON". Plasmid map based on Addgene pInducer20 (www.addgene.org/44012/)

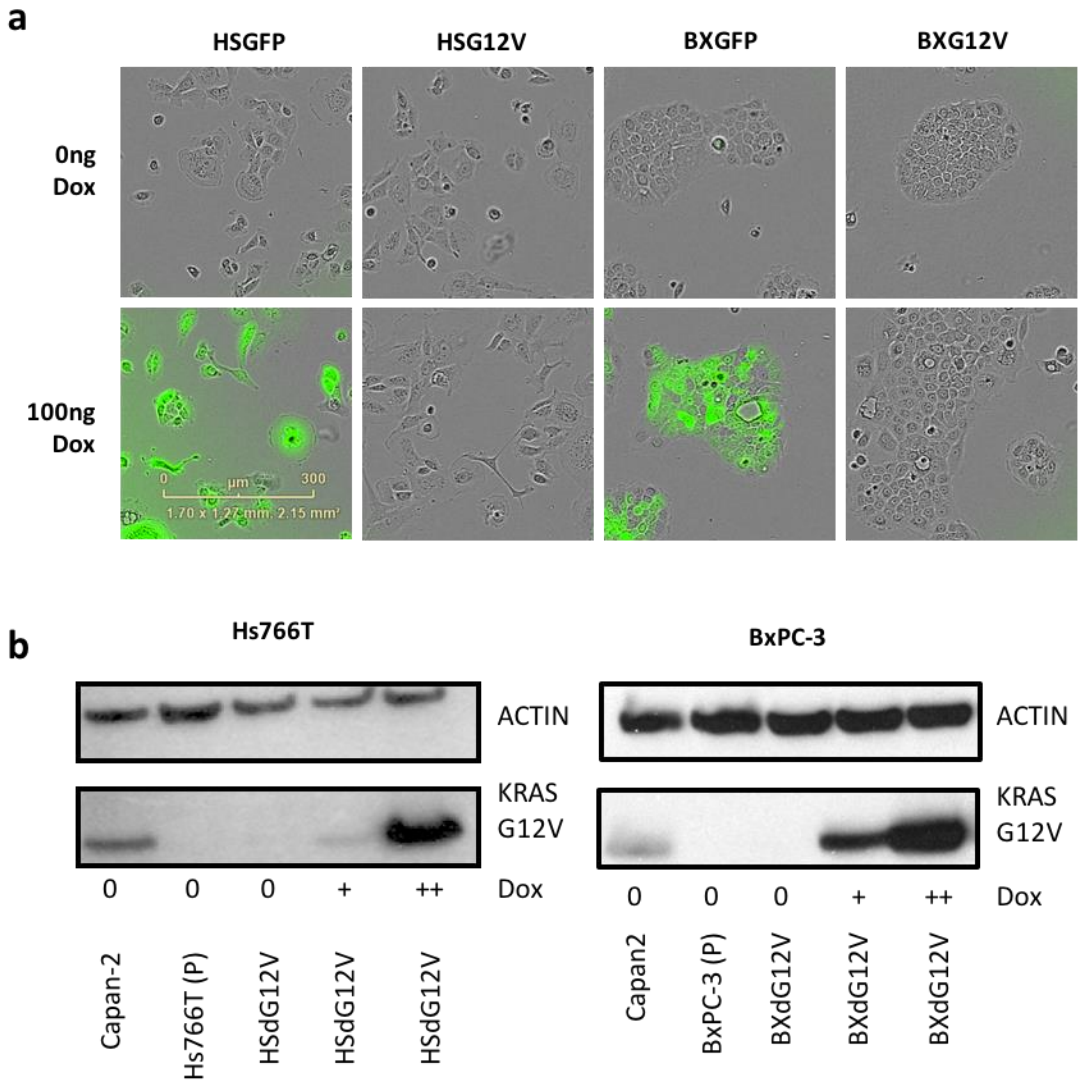

Figure 3.3: Expression validation of *KRAS* G12V model.
(**a**) Fluorescent microscopy images combined with brightfield (10X) of Dox-inducible *KRAS* G12V or *GFP* cell lines with 72 hour Dox exposure or control. (**b**) Presence of KRAS G12V was determined in Dox-inducible *KRAS* G12V cells after 72h of exposure to Dox (0-100ng) by western blot. B-actin was used as a loading control.

3.2.1.2 Transfection of Hs766T and BxPC-3 with G12D mutant *KRAS* lentiviral vectors

In addition to creating *KRAS* G12V expressing cell lines, a *KRAS* G12D isogenic cell line model was created, the most common *KRAS* mutation in PDAC [34, 35]. Purified lentiviral particles containing the *KRAS* G12D mutant, *KRAS* WT, or NTC ORFs were used to create these isogenic cell lines (Table 3.3). After antibiotic selection, transfection was further validated through the detection of GFP by fluorescent microscopy and *KRAS* expression determined by western blot. As expected, there was GFP expression in all transfected cells (Figure 3.4a). Western blot also confirmed *KRAS* G12D expression in our HSG12D and BXG12D cells and no *KRAS* G12D expression in HSNTC, HSWT, and BXNTC cells (Figure 3.4b). Together this indicates the successful transfection of *KRAS* G12D and controls into both cell lines.

Table 3.3: Summary of isogenic *KRAS* G12D model cell lines

Cell line name	Parental cell	ORF
BXG12D	BxPC-3	*KRAS* G12D
BXNTC	BxPC-3	NTC
HSWT	Hs766T	*KRAS* WT
HSG12D	Hs766T	*KRAS* G12D
HSNTC	Hs766T	NTC

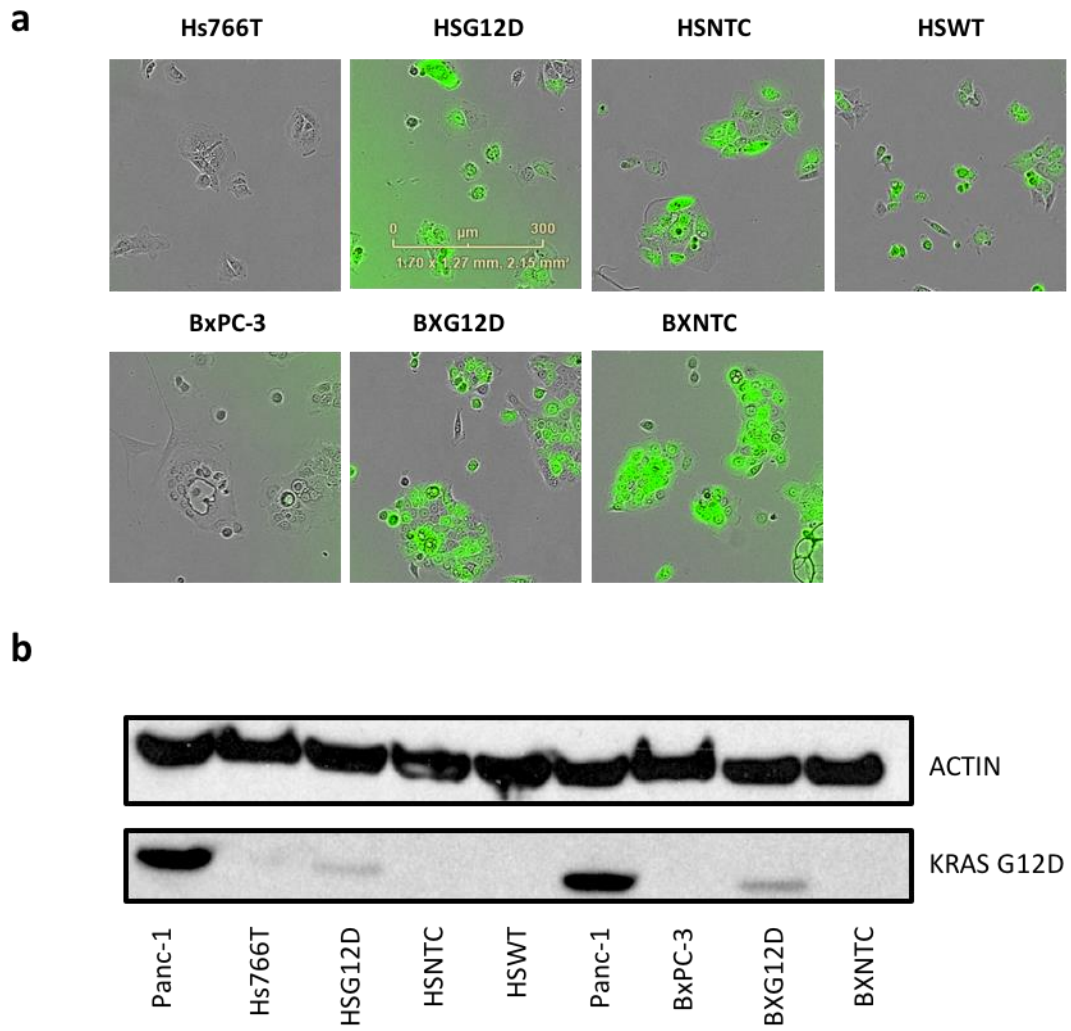

Figure 3.4: Expression validation of *KRAS* G12D model.
(**a**) Presence of GPF detected by fluorescent microscopy images combined with brightfield (10X) of parental and isogenic *KRAS* G12D, non-targetting control (NTC), and wildtype (WT) cells. (**b**) Western blot of *KRAS* G12D expression with loading control, ß-actin.

3.2.2 Vitamin C toxicity in isogenic *KRAS* mutant cell lines

After creating Hs766T and BxPC-3 cells expressing *KRAS* G12V and *KRAS* G12D proteins, susceptibility to vitamin C was determined. For the *KRAS* G12V Dox-inducible model, we tested viability after 72 hours of Dox exposure and saw no toxicity in *KRAS* G12V expressing Hs766T (HSdG12V Dox) or BxPC-3 (BXdG12V Dox) cells compared to non-expressing controls (HSdG12V, BXdG12V) or GFP expressing (HSdGFP Dox, BXdGFP Dox) and non-expressing controls (HSdGFP, BXdGFP) for doses up to 1mM vitamin C (Figure 3.5a). When testing higher doses of vitamin C (0-2.5mM) in the G12V model, toxicity occurred in all cell lines transformed with lentivirus. Thus, differences in toxicity between *KRAS* G12V expressing and non-expressing cells were undetectable (Figure 3.5b). Together these data suggest that the addition of *KRAS* G12V into Hs766T and BxPC-3 does not increase vulnerability to vitamin C at the doses tested.

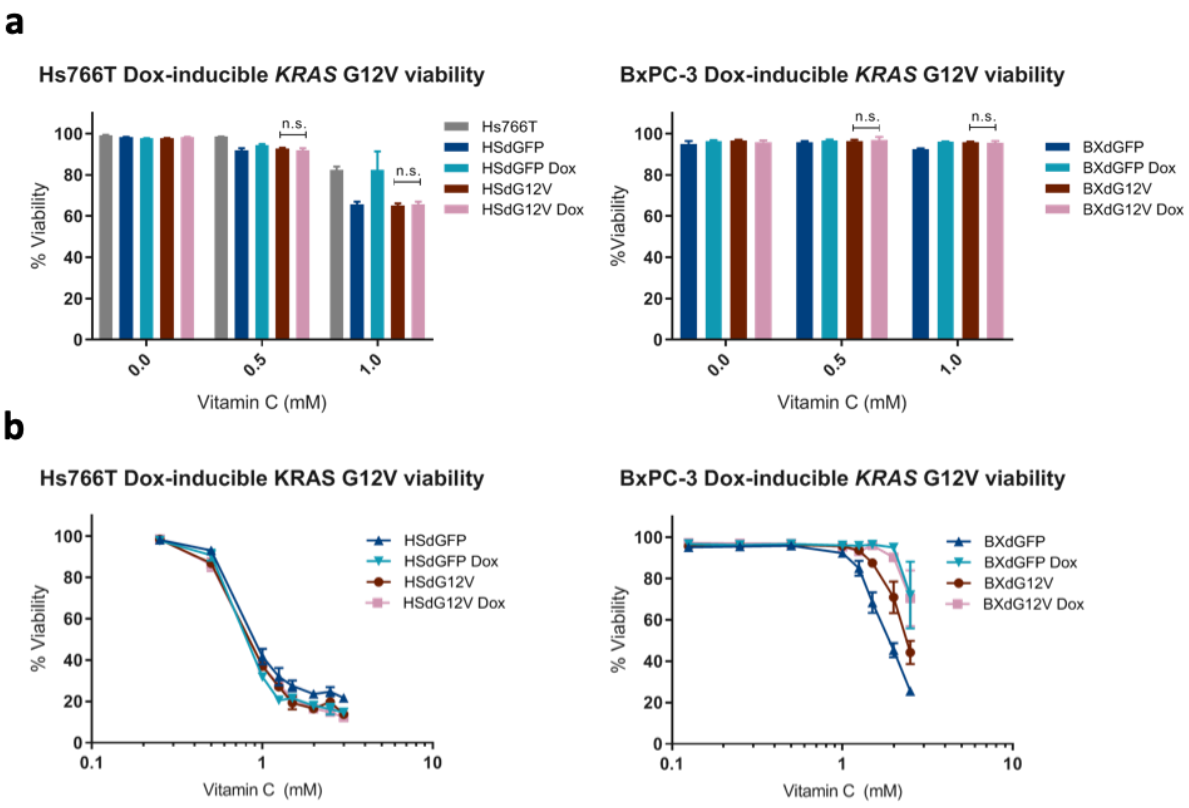

Figure 3.5: Vitamin C toxicity in Dox-inducible *KRAS* G12V cell lines
Viability results of control cells (Grey), GFP control (Blue), and *KRAS* G12V(Red) without expression (Dark shade) and with expression turned on by 72-hour exposure to Dox (Light shade). Cells were treated with (**a**) vitamin C (0-1mM) or (**b**) (0-2.5mM) for 24 hours.

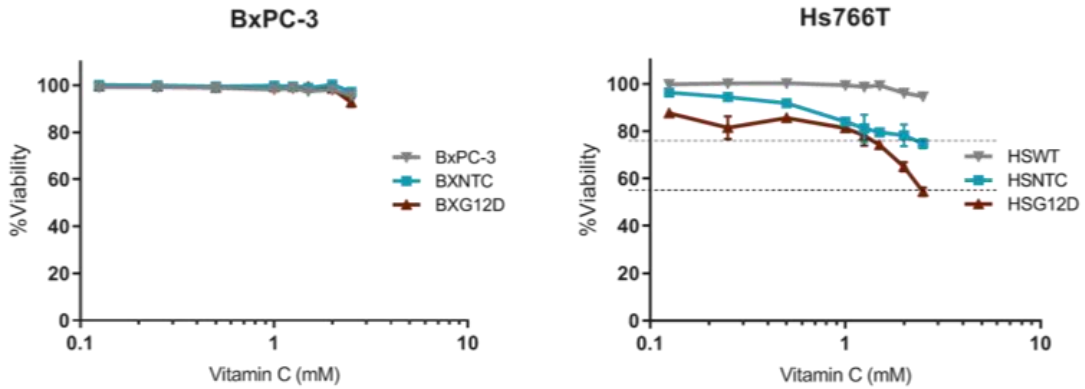

Figure 3.6: Vitamin C toxicity in *KRAS* G12D model system
Viability results of isogenic *KRAS* WT (Grey), NTC (Blue), or *KRAS* G12D (Red) cell lines treated with vitamin C (0-2.5mM) for 24 hours determined by IN Cell analysis. HSG12D vs HSNTC p=0.002 Wilcoxon matched pairs signed rank test.

In parallel to determining the viability of Dox-inducible *KRAS* G12V isogenic cell lines, vitamin C cytotoxicity was assessed in constitutively-active *KRAS* G12D isogenic cell lines. Similar to the G12V *KRAS* model, there was no observable difference in viability between *KRAS* G12D and WT BxPC-3 cells (Figure 3.6). There was however, a difference in viability between HSG12D and both HSNTC and parental controls (Figure 3.6) (HSG12D vs HSNTC p=0.002). Together, this indicates that *KRAS* G12D mutations can alter vitamin C vulnerability in some settings.

Overall, these results suggest that oncogenic *KRAS* alone may not be sufficient to induce vulnerability to vitamin C therapy in PDAC cells. In this objective, *KRAS* G12V and *KRAS* G12D were transfected into two different *KRAS* WT cell lines. Here, the Hs766T *KRAS* G12D but not BxPC-3 *KRAS* G12D or cell lines with *KRAS* G12V caused a shift in sensitivity to vitamin C. This led to the hypothesis that oncogenic KRAS can influence vitamin C sensitivity, but may work in combination with other factors either already present in the cell and/or induced by the *KRAS* mutation. As mentioned previously, preceding work has given evidence toward the interaction between vitamin C and both oxidative stress through the depletion of GSH [76, 88, 89] and glycolysis dependence [98]. Therefore, GSH levels and glycolytic dependence were explored as potential makers of vulnerability in PDAC.

3.3 Understanding the metabolic vulnerabilities to high-dose vitamin C in PDAC

The Warburg effect (first described by Otto Warburg in 1924) describes the phenomenon where cancer cells rely on aerobic glycolysis compared to oxidative phosphorylation, the preferred metabolism of normal tissues [94, 98]. More recently, driver mutations have been associated with changing the metabolisms of cancer cells. Specifically, *KRAS* mutations can cause a glycolytic switch through the Warburg effect [40-42]. Thus, I hypothesized that *KRAS*

mutant cancers that have undergone the glycolytic switch may be more vulnerable to vitamin C toxicity due to their increased dependence on glycolysis, since *KRAS* itself may not be sufficient to change vulnerability. Pancreatic cancer cell lines have previously been characterized into glycolytic and lipogenic cell types by Daeman et al. [52] in which our two highest responders in toxicity experiments were characterized as glycolytic (Table 3.4). To understand the role of glycolysis in vitamin C vulnerability in PDAC, GSH, a protein both upregulated under the glycolytic switch [93] and depleted in the mechanism of vitamin C toxicity [76, 88, 89], was examined. In addition, the effect of vitamin C on glycolysis was analyzed using the seahorse assay.

Table 3.4: Metabolic phenotype of PDAC cell lines

Cell line	Metabolic phenotype **[52]**
MIA PaCa2	Glycolytic
Panc-1	Glycolytic
Paca41.7	ND
Capan-2	Slow proliferating
BxPC-3	Lipogenic
Hs766T	Slow proliferating
HPAF-II	Lipogenic

3.3.1 Relationship between vitamin C toxicity and glutathione

Vitamin C toxicity is thought to occur by depletion of GSH [87, 90], leading to an increase in oxidative stress [94-97]. Therefore, basal levels and changes in GSH due to vitamin C were tested to determine their potential as a marker of vitamin C vulnerability in PDAC. The Promega GSH/GSSG-glow kit was used to determine glutathione levels in the cell with and without vitamin C exposure. As expected, vitamin C decreased the levels of total GSH (Figure 3.7a) and the GSH/GSSG ratio (Figure 3.7b) in all cell lines. However, Spearman's correlations indicated that basal levels of GSH, GSH/GSSG ratio, or the change in these measurements due to

vitamin C exposure did not correlate with vitamin C toxicity (Figure 3.7c-f). This suggests that while vitamin C is decreasing levels of GSH in PDAC leading to oxidative stress, the amount of GSH in the cell and the multitude of change are not associated with vulnerability to vitamin C. To validate the mechanism that GSH depletion through vitamin C induced H_2O_2 causes oxidative stress in PDAC, 5mM GSH was added to cell culture in combination with vitamin C. As expected, this resulted in a loss of vitamin C related toxicity with GSH compared to vitamin C alone (Figure 3.7g). This indicates that GSH does affect vitamin C toxicity; however, levels of GSH are not a marker of vulnerability.

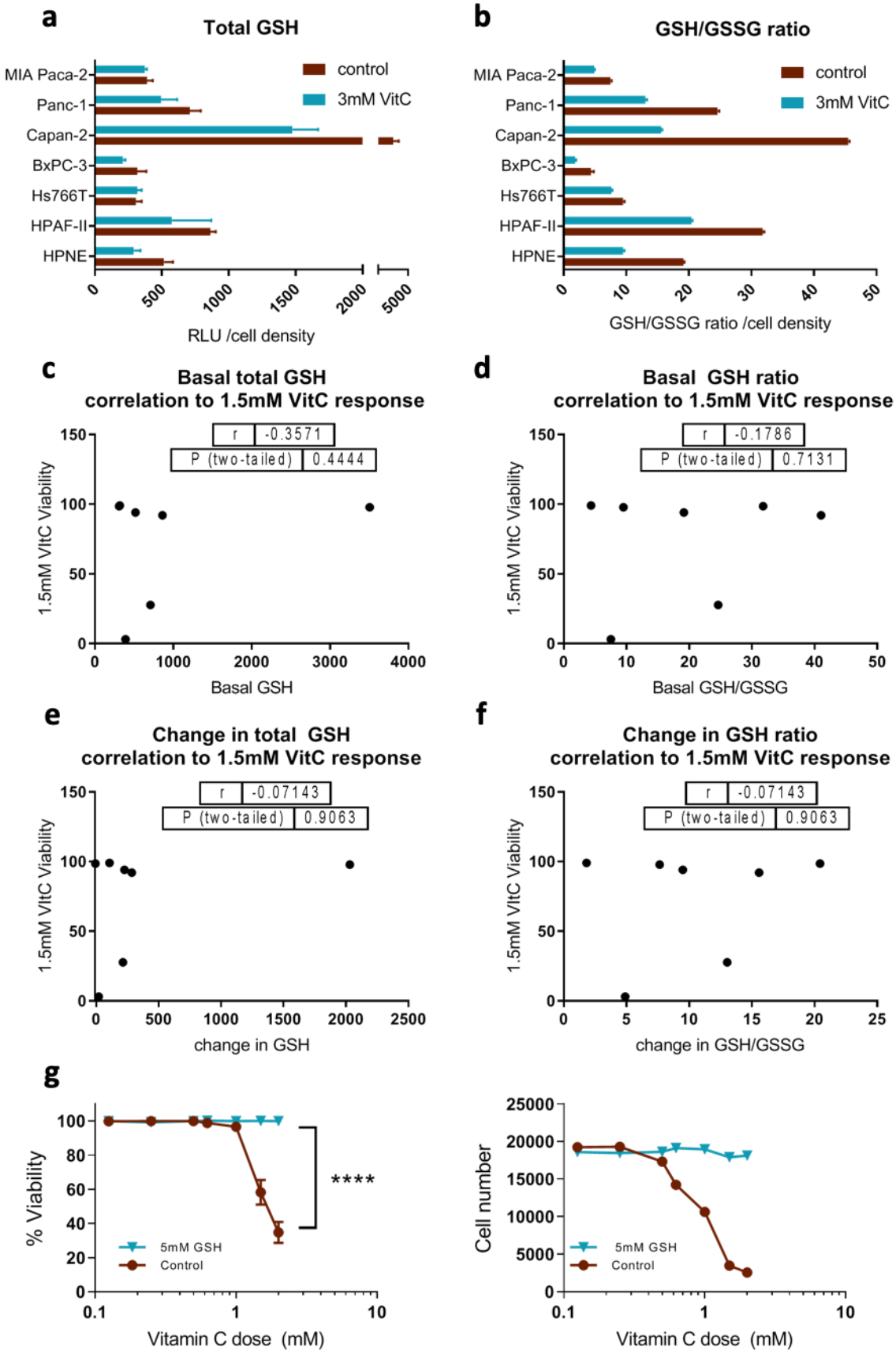
a
Total GSH
control
3mM VitC
MIA Paca-2
Panc-1
Capan-2
BxPC-3
Hs766T
HPAF-II
HPNE
0
500
1000
1500
2000
5000
RLU /cell density
b
GSH/GSSG ratio
control
3mM VitC
MIA Paca-2
Panc-1
Capan-2
BxPC-3
Hs766T
HPAF-II
HPNE
0
10
20
30
40
50
GSH/GSSG ratio /cell density
c
Basal total GSH
correlation to 1.5mM VitC response
r -0.3571
P (two-tailed) 0.4444
1.5mM VitC Viability
Basal GSH
d
Basal GSH ratio
correlation to 1.5mM VitC response
r -0.1786
P (two-tailed) 0.7131
1.5mM VitC Viability
Basal GSH/GSSG
e
Change in total GSH
correlation to 1.5mM VitC response
r -0.07143
P (two-tailed) 0.9063
1.5mM VItC Viability
change in GSH
f
Change in GSH ratio
correlation to 1.5mM VitC response
r -0.07143
P (two-tailed) 0.9063
1.5mM VItC Viability
change in GSH/GSSG
g
% Viability
****
5mM GSH
Control
Vitamin C dose (mM)
Cell number
5mM GSH
Control
Vitamin C dose (mM)

Figure 3.7: Cellular glutathione levels and relation to vitamin C toxicity.
(**a**) Bar plots indicating total glutathione (GSH) and (**b**) GSH/GSSG ratio of untreated (Red) or 3mM vitamin C (VitC) for 2 hours (Blue) detected by luminescence and normalized to cell density. No correlation between 1.5mM vitamin C viability to (**c**) basal total GSH (rho=-0.3571, p=0.4444), (**d**) basal GSH/GSSG ratio (rho=-0.1786, p=0.7131), (**e)** change in total GSH with treatment (rho=-0.07143, p=0.9063), and (**f**) change in GSH/GSSG ratio with treatment (rho=-0.07143, p=0.9063) by Spearman's correlations. (**g**) Viability and total cell number of MIA Paca-2 cells cultured in vitamin C (0-2mM) with and without 5mM GSH for 72 hours determined with IN Cell analyzer. Data was analyzed by two-way ANOVA (**** $p<0.0001$ for 1.5mM and 2mM vitamin C)

3.3.2 Analysis of glycolysis under vitamin C exposure

Results of these experiments corroborate work done by others that indicate that vitamin C toxicity is occurring through H_2O_2 induced oxidative stress [73-82]. To test whether this oxidative stress was more detrimental to glycolytic cells as previously suggested [75], and therefore a potential marker of vitamin C vulnerability, glycolysis was analyzed in both sensitive and non-sensitive cells. To determine changes in glycolysis due to vitamin C an Aligent Seahorse glycolytic stress test was performed, one of the most common methods to detect glycolysis [104]. Vitamin C decreased glycolysis in both MIA Paca-2 cells and BxPC-3 cells ($p < 0.0001$ and $p = 0.0067$, respectively) (Figure 3.8). Specifically, there was a reduction in glycolysis by 91% in MIA Paca-2 cells and by 59% in BxPC-3 cells. Although a previous study reported that vitamin C inhibits glycolysis in only vitamin C sensitive *KRAS* mutant colorectal cells compared to non-sensitive *KRAS* WT cells [87], these results depict that glycolysis is inhibited in both vitamin C sensitive, *KRAS* mutant MIA Paca-2 cells and non-sensitive, *KRAS* WT BxPC-3 cells. Previous experiments by Daemen *et al* [52] explain that cell lines reliant on the glycolytic pathway show cytotoxicity to glycolytic inhibitors where lipogenic cell lines are able to survive under glycolytic inhibition as they already prefer to use other resources for energy. Together, this indicates that pharmacological vitamin C is acting as a glycolytic inhibitor and that cell lines which are more reliant on glycolysis for energy may be more vulnerable to vitamin C due to lack of alternative energy sources.

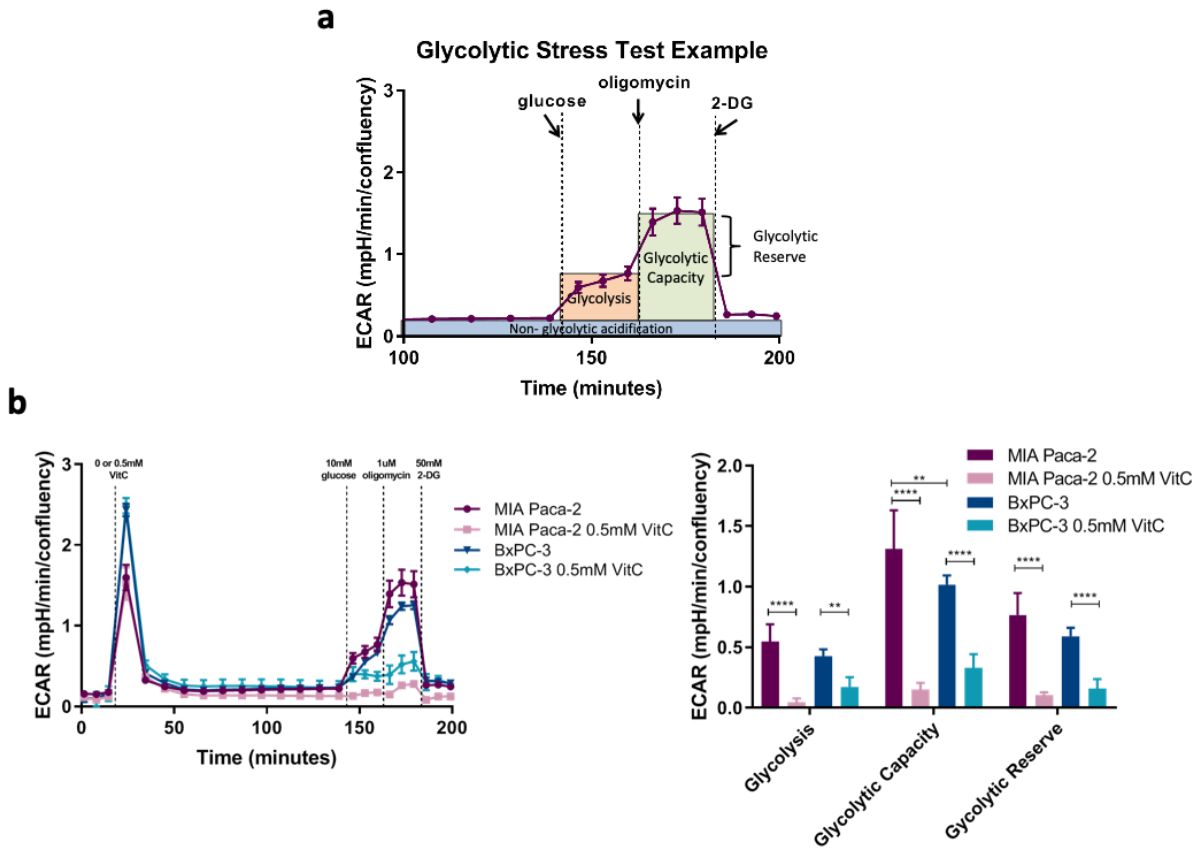

Figure 3.8: Changes in Glycolysis after vitamin C exposure.
Glycolysis was analyzed using Seahorse XFe96 glycolytic stress test. (**a**) Example of data and ranges where glycolysis, glycolytic capacity, and glycolytic reserve can be calculated. (**b**) Extracellular acidification rates (ECAR) of MIA Paca-2 and BxPC-3 of glycolytic stress test following 2-hour exposure to 0 or 0.5mM vitamin C (VitC) and normalized to well confluency determined by IncuCyte. Two-way ANOVA was used to analyze differences between treatments. ****$p < 0.0001$, **$p < 0.01$.

To further verify if dependency on glycolysis is a marker of vitamin C vulnerability, glycolytic rates were altered through glucose deprivation and subsequently vitamin C toxicity was tested. The ability of glucose concentrations to affect drug toxicity has previously been studied with metformin in relation to pancreatic cancer [105]. Specifically, culturing cells in low glucose reduced rates of glycolysis and increased rates of mitochondrial respiration [105]. Thus, I hypothesized that cells would be more vulnerable to vitamin C in high glucose conditions, where they have increased glycolysis, compared to low glucose conditions.

First, GLUT1 expression was determined by western blot. Oncogenic *KRAS* mutations are known to increase the expression of GLUT1 during the glycolytic switch [42] and the upregulation of GLUT1 expression occurs in glycolytic cell lines [70]. Differences in expression in GLUT1 between high and low glucose conditions were tested prior to determining toxicity under these conditions since GLUT1 is a transporter for both glucose and DHA. There was no significant decrease in GLUT1 in 2mM compared to 20mM glucose conditions (Figure 3.9a), indicating that potential differences in toxicity under these conditions is not due to this confounder. However, there were differences in GLUT1 levels between MIA Paca-2 and BxPC-3 cell lines, which further highlight the difference in glycolytic dependence between the two cell lines.

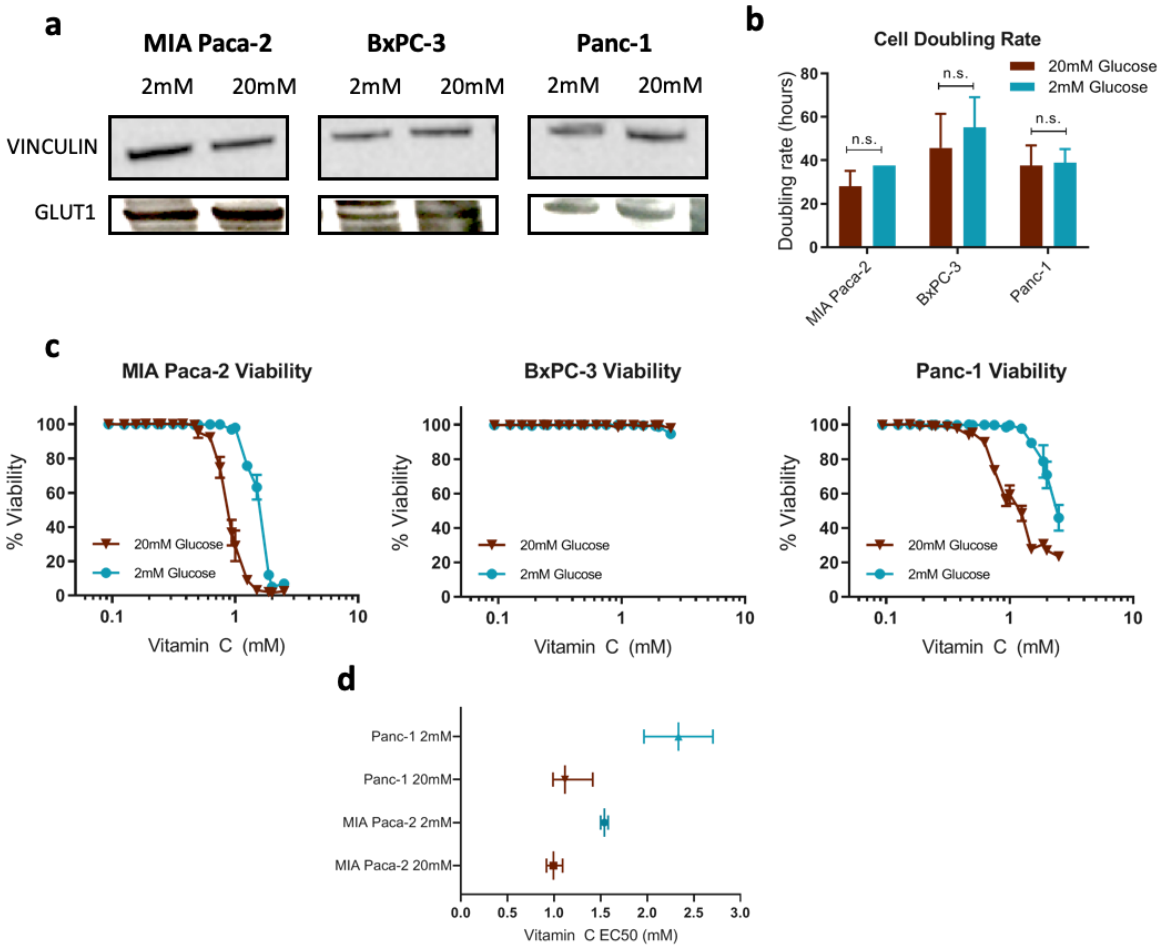

Figure 3.9: Effect of 2mM and 20mM glucose conditions on vitamin C toxicity and GLUT1 transporter.
(**a**) Western blot of GLUT1 in cell lines cultured in either 2mM or 20mM glucose containing media for 72 hours. (**b**) Bar plot indicating doubling rates of cell lines cultured in either for 72 hours in 2mM (Blue) and 20mM (Red) glucose containing media. Non-significant (n.s) based on two-way ANOVA (**c**) Viability results of PDAC cells cultured in either 2mM (Blue) or 20mM (Red) containing media for 24 hours and subsequently treated with vitamin C (0-2.5mM). Viability was then determined through IN Cell analysis. (**d**) Viability EC50s determined using non-linear fit and plotted with 95% C.I.

MIA Paca-2, BxPC-3 and Panc-1 cells were cultured in 2mM and 20mM glucose-containing DMEM and cell numbers and viability were analyzed. There were no significant differences in cell doubling time for the duration of the viability experiment (Figure 3.8b). There were, however, differences in the vitamin C EC50 in the 2mM glucose condition compared to 20mM glucose for MIA Paca-2 and Panc-1 cells (Figure 3.8c-d). Specifically, both MIA Paca-2 and Panc-1 cells needed higher concentrations of vitamin C in 2mM glucose conditions to cause toxicity compared to 20mM glucose. As expected, BxPC-3 cells which are non-sensitive at high glucose conditions, were also non-sensitive at low glucose conditions. Together, this suggests that altering glucose levels changes vitamin C vulnerability by reducing cells dependence on glycolysis; further indicating that glycolytic cells are a marker of vitamin C sensitivity.

3.4 The impact of vitamin C on PDAC patient-derived organoid models

After manipulating *KRAS* expression in immortalized cell lines and understanding the potential causes of vitamin C vulnerability in relation to glycolysis, I sought to determine the utility of vitamin C therapy in patient-derived samples with known *KRAS* mutations and expression profiles of the glycolysis pathway. To complete this objective, 3D cultures of patient-derived organoids (PDOs) from tissue collected through PANGEN (NCT02869802) were used. Beyond access to patient tissue to create PDOs, these samples also had genomic and transcriptomic data from the same tumours. The genomic and transcriptomic data provided us with the opportunity to not only test the utility of vitamin C on patient samples, but also the potential to characterize differences in toxicity pertaining to vulnerability mechanisms previously explored in cell line experiments.

Cells cultured using this 3D method, called organoids, better maintain their heterogeneity and cell-to-cell interactions observed in tumours compared to immortalized cell lines [102, 106-109]. Furthermore, organoids created with cancer patient tissue have been

documented to retain defining characteristics such as mutations, copy number alternations, and hypoxia markers [102, 108, 109]. Organoids can be established in a shorter timeframe than patient-derived mouse models [110-112] and have been used in numerous studies determining chemotherapy sensitivities and biomarker identification [107, 111, 113-116]. Our lab has created PDOs using a modified version of the Muthuswamy protocol [102] and have successfully created PDOs from xenograft tissue (xPDOs) and metastatic biopsy tissue (mPDOs). IN Cell analysis was optimized to detect cells in a matrigel coated plate, which allows high throughput screening by staining live and dead cells. Due to their nature, 3D models need up to 3 magnitudes higher dose than their 2D counterparts for comparable toxicity [106, 117]. Therefore, vitamin C and gemcitabine doses and the staining protocol were optimized prior to testing PDOs, as described below.

3.4.1 Toxicity of vitamin C in patient-derived organoids

To determine whether vitamin C is toxic to patient-derived models, four mPDO cell lines were used (Figure 3.10a) (Table 3.5). After exposure to vitamin C, cell viability was determined and toxicity was observed in all mPDOs tested **(**Figure 3.10b). Interestingly, there were varying degrees of toxicity among the organoid lines, but a larger sample size would be needed to determine differences in glycolysis between lines that could be leading to vulnerability. In our cohort it was also observed that vitamin C is toxic to both gemcitabine sensitive and resistant PDOs (Figure 3.10c-d), indicating the potential of vitamin C therapy for gemcitabine resistant PDAC.

Table 3.5: Patient-derived organoid tissue characteristics

Sample	**mPDO9**	**mPDO18**	**mPDO20**	**mPDO22**	**xPDO41**
KRAS	G12V (cg)	Q61H (cg)	G12D (nd)	G12D	G12V (nd)
MCT4 expression	53rd percentile	90th percentile	nd	40th percentile	nd
GLUT1 expression	77th percentile	90th percentile	nd	27th percentile	nd
MYC expression	36th percentile	64th percentile	nd	94th percentile	nd
MYC amplification	Copy neutral	One copy gain	nd	Copy neutral	nd
Metabolic Subtype	Glycolytic	Cholesterogenic	nd	Mixed	nd
Moffit subtype	Basal-like	Basal-like	nd	Classical	nd
Bailey Subtype	Squamous	Squamous	nd	Squamous	nd
Collisson Subtype	Quasi-mesenchymal	Classical	nd	Classical	nd

*copy gain=cg, not determined=nd

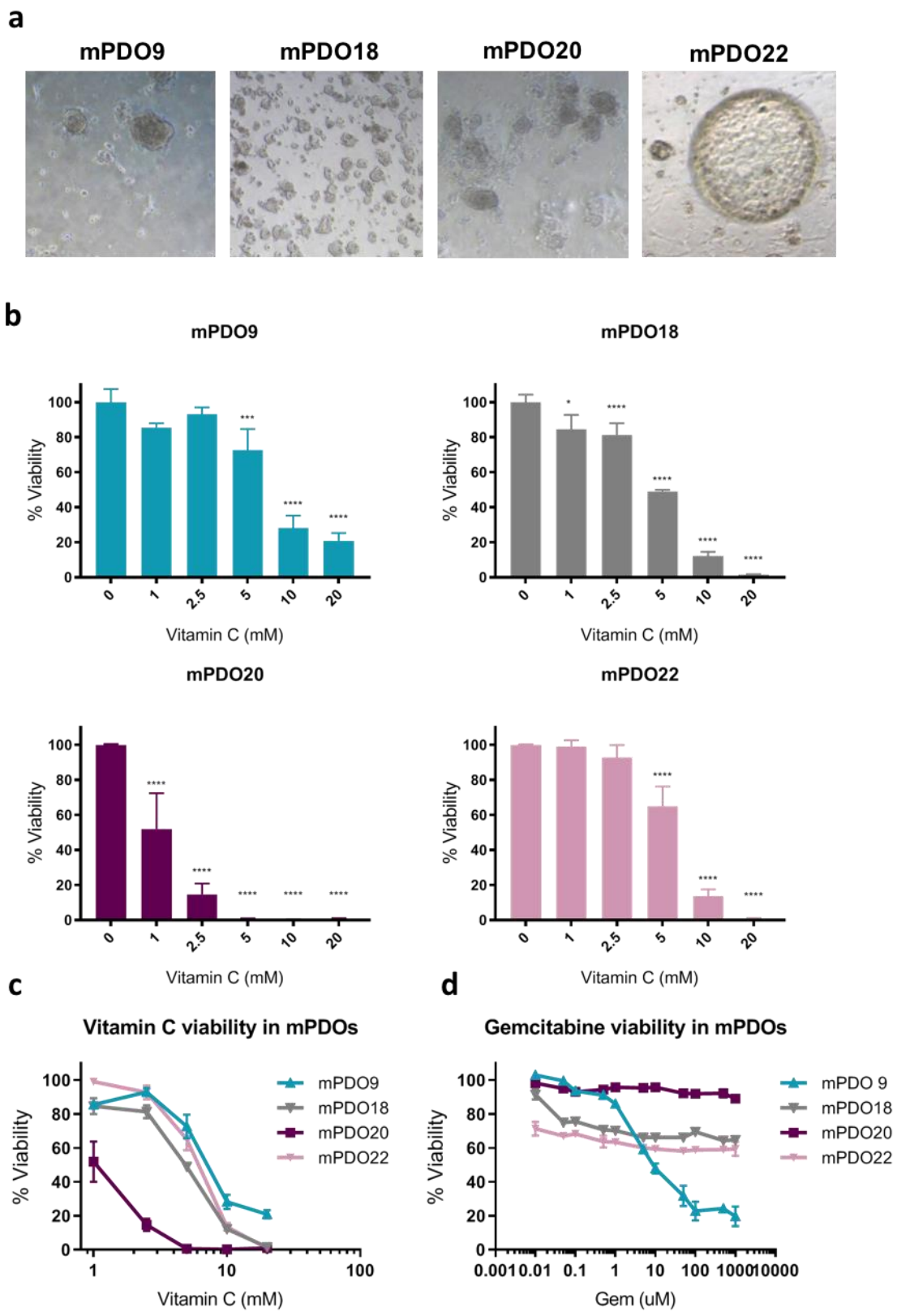
a
mPDO9
mPDO18
mPDO20
mPDO22
b
mPDO9
mPDO18
mPDO20
mPDO22
% Viability
Vitamin C (mM)
0
1
2.5
5
10
20
c
Vitamin C viability in mPDOs
mPDO9
mPDO18
mPDO20
mPDO22
Vitamin C (mM)
d
Gemcitabine viability in mPDOs
mPDO 9
mPDO18
mPDO20
mPDO22
Gem (uM)

Figure 3.10: Toxicity of vitamin C and Gemcitabine in PDOs.
(**a**) Cell viability results of organoids were treated with vitamin C (0-20mM) for 72 hours prior to IN Cell analysis. Viability normalized to untreated control. Differences in viability were compared to untreated controls by two-way ANOVA Tukey's multiple comparisons (*p<0.1, ***p<0.001, ****p<0.0001). (**b**) Cell viability results of xPDO41 treated with vitamin C (1-20mM) either alone or in combination with gemcitabine (Gem) for 72 hours prior to staining and analysis. Viability was normalized to untreated control. Differences in viability were compared to respective vitamin C untreated controls by two-way ANOVA Tukey's multiple comparisons. (**c**) Viability of organoids treated with Gem (0-1mM) for 72 hours prior to staining and IN Cell analysis. Viability was normalized to vehicle control.

Beyond vitamin C as a single agent therapy, it was important to understand the effect of vitamin C in combination with chemotherapy. In order to target multiple pathways and cancer cells, therapies are often administered in combination rather than as a single [118]. Furthermore, patients participating in clinical trials will typically receive new treatments in combination with standard of care treatment regimens [118]. Therefore, to understand the utility of vitamin C therapy, it was critical to test vitamin C in combination with gemcitabine. While both were effective as single agents in our model, there was a greater toxicity when vitamin C was used with gemcitabine (Figure 3.11a). Previous studies reported similar findings that vitamin C and gemcitabine are synergistic in cell line and mouse models [119, 120]. Reports have suggested that while vitamin C does not reduce gemcitabine toxicity, gemcitabine does reduce vitamin C toxicity in combination compared to vitamin C alone [61]. Congruent to these finding, my results indicate that vitamin C in combination with a low dose of gemcitabine causes greater toxicity than vitamin C with a high dose of gemcitabine ($p = 0.0068$) (Figure 3.11b). Together this data indicates that vitamin C may be a useful therapy both in combination with first line therapy or as an adjuvant therapy after chemotherapy resistance occurs. Overall this data using patient-derived models shows the utility of pharmacological vitamin C treatment.

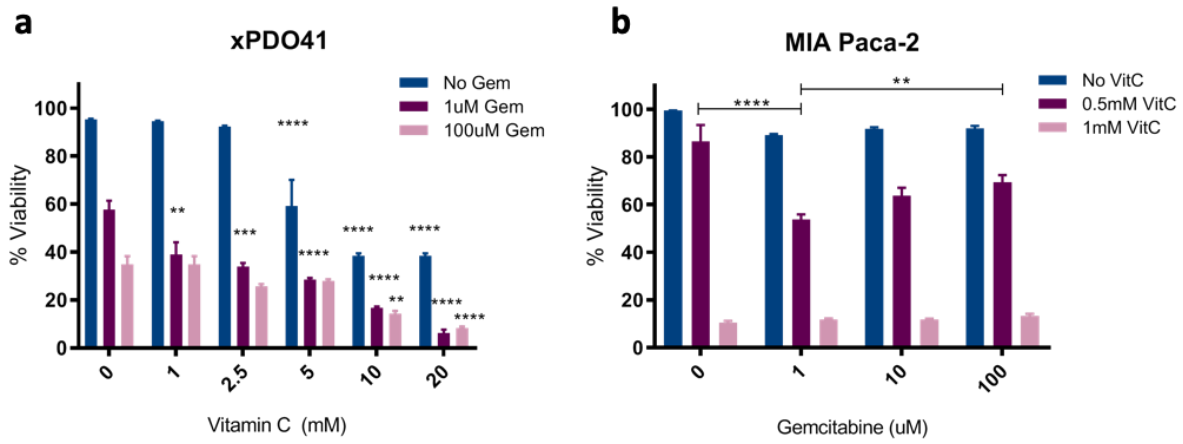

Figure 3.11: Combination treatment of vitamin C and gemcitabine
(**a**) Cell viability results of xPDO41 treated with vitamin C (1-20mM) either alone or in combination with gemcitabine (Gem) for 72 hours prior to staining and analysis. Viability was normalized to untreated control. Differences in viability were compared to respective vitamin C untreated controls by two-way ANOVA Tukey's multiple comparisons. (**b**) Cell viability results of MIA Paca-2 treated with gemcitabine (0-100µM) either alone or in combination with vitamin C (VitC) for 72 hours prior to staining and analysis. Viability was normalized to untreated control. Differences in viability were compared by two-way ANOVA Tukey's multiple comparisons. (*p<0.1, **p<0.01) ***p<0.001, ****p<0.0001

Chapter 4: Discussion

4.1 Summary of research

Pancreatic ductal adenocarcinoma is a deadly disease with few markers of susceptibility to the limited treatment options. Therefore, I sought to determine if pharmacological vitamin C, a treatment recently rediscovered as a potential cancer treatment, has clinical utility for PDAC patients with the focus of determining a marker of vulnerability to this treatment. After testing a panel of PDAC cell lines, I determined differences in susceptibility to vitamin C at the doses tested. Due to crystallization confounding IN Cell analysis, I used lower vitamin C doses than other groups [73, 75, 79, 80, 87, 90]. Higher doses may have caused toxicity in all cell lines tested, however, caused toxicity to non-malignant cell lines. Testing non-malignant cell lines, determined that that the doses I used with IN Cell (0-2.5mM) reached the maximum of the therapeutic window, which were doses non-toxic to the non-malignant cells. While I did not test doses as high as other groups, I found that cytotoxicity in cell lines occurs beyond 0.5mM with EC50s of approximately 1mM for the sensitive cell lines (MIA Paca-2 and Panc-1), consistent with another PDAC cell study [90]. Previous vitamin C cytotoxicity studies in PDAC cell lines found EC50s of approximately 1mM in MIA Paca-2 and Panc-1 cells [90] and studies in other cancer cell types found EC50s ranging from 1-7mM [73, 75, 79, 80, 87, 90]. Any variability observed in EC50s were likely due to differences in assays. Many groups used the MTT assay [75, 79, 80, 90], which as mentioned previously, can be confounded when used with vitamin C [103].

Based on previous research indicating that *KRAS* mutations infer vitamin C vulnerability in colorectal cancer [87] and the results from our panel proposing that *KRAS* mutant PDAC cells were more sensitive than *KRAS* WT cells, I created two isogenic cell line models expressing either *KRAS* G12V or *KRAS* G12D mutant proteins. Based on the resources available, our two

model systems used differing methods of expression. Our G12V lentivirus vectors were generously donated by Dr. Lockwood and used a Dox-inducible system for *KRAS* expression. In contrast our G12D lentivirus model used a constitutively active promoter for *KRAS* expression. Using these two different systems limits our ability to compare the results of both systems directly, but using Dr. Lockwood's resources enabled the creation of the G12V modeling system. Together, these systems captured the two most prevalent *KRAS* mutations in PDAC [34, 35]. While a constitutively active expression system may be the most useful for my current studies as it allows the cells to adapt to the mutant KRAS, other experiments can benefit from a Dox-inducible model to detect these adaptations over time and subsequent KRAS deprivation.

Testing our two isogenic *KRAS* mutant model systems resulted in increased sensitivity in the HSG12D cell line, but none of the other cell lines created. Beyond differences in the two modeling systems described above, there could be other reasons to explain the differing results between cell lines and between *KRAS* mutations. For instance, besides both being *KRAS* WT, the genetic background between Hs766T and BxPC-3 differs. One example is that Hs766T has WT *TP53* whereas BxPC-3 has a *TP53* mutation. These differences along with others, could explain why KRAS G12D increased sensitivity in Hs766T but not in BxPC-3. These results suggest that factors beyond *KRAS* mutations alone may be needed in the cell for mutant KRAS to cause specific downstream effects that create vulnerability to vitamin C.

It is also known that not all *KRAS* mutations are equal and specific amino acid changes can alter the protein in different ways, which leads to differential expression downstream of KRAS [35, 42, 43, 45, 121, 122]. Therefore, the effects of *KRAS* G12D may be more likely to induce the changes needed for vitamin C vulnerability. As mentioned previously, *KRAS* mutations are known to alter metabolism, causing an increase in glycolysis [40-42]. Interestingly, current research indicates that the *KRAS* G12D mutation may be the biggest driver

of the RAS-driven glycolytic switch, compared to other *KRAS* mutations [42, 45]. This expression pattern difference between *KRAS* G12D compared to *KRAS* G12V may explain why the G12D mutation caused a difference in sensitivity to vitamin C in HS766T while the G12V mutation did not.

Overall, these results do not depict that *KRAS* mutation status is an indicator of vitamin C vulnerability, as originally hypothesized. Differences in the effect of *KRAS* integration between cell lines and the two *KRAS* mutations suggests that *KRAS* alone does not induce vitamin C vulnerability, but rather supports the notion that *KRAS* mutations in relation to glycolysis and glycolytic switch may be a marker of vitamin C susceptibility. This hypothesis was tested using two potential markers: glutathione levels, a molecule used in glycolysis, upregulated under the glycolytic switch, and depleted in the mechanism of vitamin C toxicity; and glycolytic rates.

Previous mechanistic studies have indicated that H_2O_2 causes toxicity through increased ROS [73-82] and that both DHA and H_2O_2 decreased levels of GSH [88-90], leading to cell death. Therefore, I was interested in whether cells with higher levels of GSH were more protected from vitamin C toxicity. Results of testing basal GSH levels, changes in GSH levels due to vitamin C exposure, the ratio of GSH/GSSG both at basal conditions and under vitamin C exposure, and comparison of these levels against vitamin C toxicity indicated that GSH is not a marker of vitamin C exposure. However, results depicted that vitamin C decreases GSH levels in all cells, consistent with other studies [88-90]. Furthermore, when GSH, a H_2O_2 scavenger [87], was added in combination with vitamin C, no toxicity was observed. While GSH levels are not a marker of sensitivity to vitamin C, these data support the mechanism of vitamin C toxicity previously suggested for solid tumours [73-82, 87-90].

Other groups have suggested that vitamin C vulnerability in ovarian cancer may be related to glycolysis since glycolytic cells may be more vulnerable to H_2O_2 toxicity [75]. Our

results further advocate the potential of glycolysis as a marker of vulnerability and necessitates the exploration of glycolysis and vitamin C toxicity. Thus, glycolysis and changes in glycolysis due to vitamin C were determined in a vitamin C responsive, *KRAS* mutant cell line, MIA Paca-2, and vitamin C non-responsive, KRAS WT cell line, BxPC-3. When Yun et al. [87] performed a similar study, glycolysis was only inhibited in their vitamin C sensitive cells, however my results argue that vitamin C inhibits glycolysis regardless of vitamin C induced toxicity. This selective toxicity due to glycolysis inhibition has been previously studied. Experiments done by Daeman et al. [52] indicated that cells which are dependent on glycolysis are more susceptible to glycolytic inhibitors than lipogenic cell lines and vice versa. Interestingly, the two most responsive cell lines (MIA Paca-2, and Panc-1) were characterized as glycolytic and the non-responsive cell lines were characterized as either lipogenic (HPAF-II and BxPC-3) or slow growing (Capan-2 and Hs766T) [52]. Work by Daeman et al. [52] supports my findings, which suggests that while vitamin C is acting as a glycolytic inhibitor in both lipogenic BxPC-3 and glycolytic MIA Paca-2 lines, vitamin C is selectively toxic to the glycolytic dependant cells. Overall this indicates that highly glycolytic cell lines may be a marker of vitamin C vulnerability.

Since pharmacological vitamin C toxicity inhibits glycolysis and leads to cell death in glycolytic cell lines, I tested whether reducing glycolytic rates would alter vitamin C sensitivity. This experiment used a previously employed strategy used to study metformin sensitivity where low glucose conditions were used to reduce glycolytic rates in PDAC cell lines [105]. As expected, cells were less sensitive to vitamin C when cultured under low glucose conditions. Glycolytic rates under high and low glucose conditions require further testing to confirm whether differences in toxicity are a result of lowered glycolytic rates. The data presented in this thesis, however, indicates a potential application of vitamin C treatment for glycolytic cell lines and should be explored in future studies.

While cell lines are an important tool in cancer research, many findings in immortalized cell lines do not translate well into humans [123] likely due to their differential expression patterns compared to patient-derived models [16]. As a step towards clinical models, patient-derived organoids were used to determine whether vitamin C toxicity occurs in a more representative model of PDAC tumours. This resulted in toxicity in five PDO models when tested at doses which are achievable in the clinic. However, since there is not a non-malignant organoid control available, knowing whether this toxicity occurs within the therapeutic window for this model is undeterminable. Nevertheless, there was differential toxicity among organoids with mPDO20 showing toxicity at 1mM vitamin C which is within the therapeutic window of cell lines. Since higher drug concentrations are needed in organoid models [106, 117] it can be inferred that this line is in fact susceptible to vitamin C at doses unlikely to affect non-malignant organoids. Others have also shown that pharmacological vitamin C is toxic to patient-derived cell and murine models [75, 87]. However, this is the first known use of organoids and vitamin C vulnerability, presenting a new tool to test vitamin C vulnerability in patient-derived samples.

As new therapies are often given in combination with standard of care, organoids were treated with vitamin C and gemcitabine. When testing vitamin C in combination with gemcitabine there was an increase in toxicity compared to either agent alone and toxicity occurred in both gemcitabine resistant and sensitive cell lines. Other groups went beyond determining synergy and established that pharmacological vitamin C does not affect the pharmacokinetics of gemcitabine *in vivo* [61], meaning that vitamin C will not diminish gemcitabine treatment. Interestingly, they found that gemcitabine increased the clearance rate of vitamin C, likely lowering the toxicity of vitamin C when given with gemcitabine compared to monotherapy [61]; which is consistent with my results indicating that vitamin C and gemcitabine are synergistic and cause greater toxicity in combination with a low gemcitabine dose compared

to a high dose. These results demonstrate that using a combination treatment of vitamin C and gemcitabine may have clinical utility and that vitamin C monotherapy could be a beneficial treatment for those resistant to other treatment options.

4.2 Significance

In this thesis, the role of both *KRAS* and glycolysis were investigated to understand differences in vitamin C sensitivity for PDAC. I observed that oncogenic *KRAS* does not infer vitamin C sensitivity; however, oncogenic *KRAS* may promote sensitivity through upregulation of glycolysis, which I propose is a marker of vitamin C vulnerability. Groups have shown that the majority of PDAC cases are highly glycolytic [16] and vitamin C therapy may be beneficial to a large portion of PDAC patients. Furthermore, gemcitabine resistant cancers often have a glycolytic phenotype [124]. With the growing rates of PDAC patients, large portions of glycolytic subtypes, and increased rates of this aggressive subtype after gemcitabine treatment there is a growing need for therapies targeting glycolytic PDAC. Metabolic pathways are an increasingly popular research area in pancreatic cancer with many groups working to understand the metabolic subtypes and cell signalling pathways which drive metabolic subtypes [16, 47, 49, 50]. Moreover, these studies have led to many experimental inhibitors and drugs that have been used to inhibit parts of the glycolytic pathway, including GLUT1, MCT1, PKM2, GAPDH, and hexokinase [125, 126]. These compounds, however, have either not reached clinical trials or failed clinical trials due to low specificity, off target effects, and toxicities [125, 126]. Therefore, there is still an unmet need for therapies that safely and effectively target glycolysis.

Pharmacological vitamin C causes toxicity through the mechanism of H_2O_2 induced toxicity, inhibiting glycolysis. Unlike other glycolytic inhibitors, vitamin C toxicity is selective to cancer cells due to the non-direct inhibition of glycolysis. Vitamin C causes the accumulation of H_2O_2, which normal cells are more effective at removing [81], allowing for the use of high

concentrations. Furthermore, pharmacological vitamin C is already proven to be safe in cancer patients with no serious adverse events and there are ongoing trials to determine efficacy. Pharmacological vitamin C shows promise as being an agent to target this highly aggressive, cancer promoting pathway; moreover, high glycolytic phenotypes may predict response to vitamin C in PDAC and could be used as a marker to select patients for clinical trials to aid in analysis of clinical efficacy.

4.3 Future Directions

Although it is recognized that vitamin C influences metabolism, increased sensitivity in glycolytic subtypes has yet to be validated. To further test this hypothesis, analyzing glycolysis rates and proteins downstream of KRAS in our isogenic *KRAS* G12D and G12V models may elucidate the changes that only occurred in the vitamin C vulnerable HSD12D cell line. Furthermore, while low glucose conditions were used to alter glycolysis rates and evaluate the resulting changes in sensitivity, other glycolytic activators and inhibitors could be used to manipulate cells or organoids to determine changes in sensitivity to vitamin C as a result of changes in glycolysis.

While validating the role of glycolysis in these cell models will strengthen the argument that glycolytic cell lines are a marker of vitamin C therapy, tools that aid in the development of this marker in the clinic are critical. Now that the protocols are in place for testing vitamin C sensitivity in PDOs, continued testing of these models, which have matched patient genomic and transcriptomic data, may present an opportunity to create single or multigene panels. The creation of these panels would allow for metabolic subtype determination using a feasible clinical tool. MCT4 and c-MYC have been associated with glycolytic tumours [127, 128] and could be potential genes to identify within our PDO models. Furthermore, these could be a used

to determine metabolic subtypes in ongoing clinical trials using pharmacological IV vitamin C treatment to stratify response.

References

1. *Canadian Cancer Statistics 2017*, Canadian Cancer Society: Toronto, ON.
2. Siegel, R.L., K.D. Miller, and A. Jemal, *Cancer statistics, 2018.* CA Cancer J Clin, 2018. **68**(1): p. 7-30.
3. Siegel, R.L., K.D. Miller, and A. Jemal, *Cancer statistics, 2015.* CA Cancer J Clin, 2015. **65**(1): p. 5-29.
4. Siegel, R., D. Naishadham, and A. Jemal, *Cancer statistics, 2013.* CA Cancer J Clin, 2013. **63**(1): p. 11-30.
5. Rahib, L., et al., *Projecting cancer incidence and deaths to 2030: the unexpected burden of thyroid, liver, and pancreas cancers in the United States.* Cancer Res, 2014. **74**(11): p. 2913-21.
6. Waddell, N., et al., *Whole genomes redefine the mutational landscape of pancreatic cancer.* Nature, 2015. **518**(7540): p. 495-501.
7. Biankin, A.V., et al., *Pancreatic cancer genomes reveal aberrations in axon guidance pathway genes.* Nature, 2012. **491**(7424): p. 399-405.
8. Jiao, Y., et al., *DAXX/ATRX, MEN1, and mTOR pathway genes are frequently altered in pancreatic neuroendocrine tumors.* Science, 2011. **331**(6021): p. 1199-203.
9. Donahue, T.R. and D.W. Dawson, *Leveraging Mechanisms Governing Pancreatic Tumorigenesis To Reduce Pancreatic Cancer Mortality.* Trends Endocrinol Metab, 2016. **27**(11): p. 770-781.
10. Lee, A.Y.L., et al., *Cell of origin affects tumour development and phenotype in pancreatic ductal adenocarcinoma.* Gut, 2018.
11. Iacobuzio-Donahue, C.A., et al., *Genetic basis of pancreas cancer development and progression: insights from whole-exome and whole-genome sequencing.* Clin Cancer Res, 2012. **18**(16): p. 4257-65.
12. Kleeff, J., et al., *Pancreatic cancer.* Nat Rev Dis Primers, 2016. **2**: p. 16022.
13. Makohon-Moore, A. and C.A. Iacobuzio-Donahue, *Pancreatic cancer biology and genetics from an evolutionary perspective.* Nat Rev Cancer, 2016. **16**(9): p. 553-65.
14. Mollenhauer, J., I. Roether, and H.F. Kern, *Distribution of extracellular matrix proteins in pancreatic ductal adenocarcinoma and its influence on tumor cell proliferation in vitro.* Pancreas, 1987. **2**(1): p. 14-24.
15. Sato, N., N. Maehara, and M. Goggins, *Gene expression profiling of tumor-stromal interactions between pancreatic cancer cells and stromal fibroblasts.* Cancer Res, 2004. **64**(19): p. 6950-6.
16. Moffitt, R.A., et al., *Virtual microdissection identifies distinct tumor- and stroma-specific subtypes of pancreatic ductal adenocarcinoma.* Nat Genet, 2015. **47**(10): p. 1168-78.
17. Provenzano, P.P., et al., *Enzymatic targeting of the stroma ablates physical barriers to treatment of pancreatic ductal adenocarcinoma.* Cancer Cell, 2012. **21**(3): p. 418-29.
18. Lei, J., et al., *Hedgehog signaling regulates hypoxia induced epithelial to mesenchymal transition and invasion in pancreatic cancer cells via a ligand-independent manner.* Mol Cancer, 2013. **12**: p. 66.
19. Yuen, A. and B. Diaz, *The impact of hypoxia in pancreatic cancer invasion and metastasis.* Hypoxia (Auckl), 2014. **2**: p. 91-106.
20. *Canadian Cancer Statistics 2018*, Canadian Cancer Society: Toronto, ON.
21. Stathis, A. and M.J. Moore, *Advanced pancreatic carcinoma: current treatment and future challenges.* Nat Rev Clin Oncol, 2010. **7**(3): p. 163-72.

22. Butturini, G., et al., *Influence of resection margins and treatment on survival in patients with pancreatic cancer: meta-analysis of randomized controlled trials.* Arch Surg, 2008. **143**(1): p. 75-83; discussion 83.
23. Spanknebel, K. and K.C. Conlon, *Advances in the surgical management of pancreatic cancer.* Cancer J, 2001. **7**(4): p. 312-23.
24. He, J., et al., *2564 resected periampullary adenocarcinomas at a single institution: trends over three decades.* HPB (Oxford), 2014. **16**(1): p. 83-90.
25. Whiteman, D.C., et al., *Cancers in Australia in 2010 attributable to modifiable factors: introduction and overview.* Aust N Z J Public Health, 2015. **39**(5): p. 403-7.
26. Bosetti, C., et al., *Cigarette smoking and pancreatic cancer: an analysis from the International Pancreatic Cancer Case-Control Consortium (Panc4).* Ann Oncol, 2012. **23**(7): p. 1880-8.
27. Lowenfels, A.B., et al., *Hereditary pancreatitis and the risk of pancreatic cancer. International Hereditary Pancreatitis Study Group.* J Natl Cancer Inst, 1997. **89**(6): p. 442-6.
28. Bosetti, C., et al., *Diabetes, antidiabetic medications, and pancreatic cancer risk: an analysis from the International Pancreatic Cancer Case-Control Consortium.* Ann Oncol, 2014. **25**(10): p. 2065-72.
29. Burris, H.A., 3rd, et al., *Improvements in survival and clinical benefit with gemcitabine as first-line therapy for patients with advanced pancreas cancer: a randomized trial.* J Clin Oncol, 1997. **15**(6): p. 2403-13.
30. Cunningham, D., et al., *Phase III randomized comparison of gemcitabine versus gemcitabine plus capecitabine in patients with advanced pancreatic cancer.* J Clin Oncol, 2009. **27**(33): p. 5513-8.
31. Moore, M.J., et al., *Erlotinib plus gemcitabine compared with gemcitabine alone in patients with advanced pancreatic cancer: a phase III trial of the National Cancer Institute of Canada Clinical Trials Group.* J Clin Oncol, 2007. **25**(15): p. 1960-6.
32. Von Hoff, D.D., et al., *Increased survival in pancreatic cancer with nab-paclitaxel plus gemcitabine.* N Engl J Med, 2013. **369**(18): p. 1691-703.
33. Conroy, T., et al., *FOLFIRINOX versus gemcitabine for metastatic pancreatic cancer.* N Engl J Med, 2011. **364**(19): p. 1817-25.
34. Cancer Genome Atlas Research Network. Electronic address, a.a.d.h.e. and N. Cancer Genome Atlas Research, *Integrated Genomic Characterization of Pancreatic Ductal Adenocarcinoma.* Cancer Cell, 2017. **32**(2): p. 185-203 e13.
35. Cox, A.D., et al., *Drugging the undruggable RAS: Mission possible?* Nat Rev Drug Discov, 2014. **13**(11): p. 828-51.
36. Hobbs, G.A., C.J. Der, and K.L. Rossman, *RAS isoforms and mutations in cancer at a glance.* J Cell Sci, 2016. **129**(7): p. 1287-92.
37. Bryant, K.L., et al., *KRAS: feeding pancreatic cancer proliferation.* Trends Biochem Sci, 2014. **39**(2): p. 91-100.
38. Eser, S., et al., *Oncogenic KRAS signalling in pancreatic cancer.* Br J Cancer, 2014. **111**(5): p. 817-22.
39. Jancik, S., et al., *Clinical relevance of KRAS in human cancers.* J Biomed Biotechnol, 2010. **2010**: p. 150960.
40. Kawada, K., K. Toda, and Y. Sakai, *Targeting metabolic reprogramming in KRAS-driven cancers.* Int J Clin Oncol, 2017. **22**(4): p. 651-659.
41. Son, J., et al., *Glutamine supports pancreatic cancer growth through a KRAS-regulated metabolic pathway.* Nature, 2013. **496**(7443): p. 101-5.

42. Ying, H., et al., *Oncogenic Kras maintains pancreatic tumors through regulation of anabolic glucose metabolism.* Cell, 2012. **149**(3): p. 656-70.
43. Ihle, N.T., et al., *Effect of KRAS oncogene substitutions on protein behavior: implications for signaling and clinical outcome.* J Natl Cancer Inst, 2012. **104**(3): p. 228-39.
44. Ogura, T., et al., *Prognostic value of K-ras mutation status and subtypes in endoscopic ultrasound-guided fine-needle aspiration specimens from patients with unresectable pancreatic cancer.* J Gastroenterol, 2013. **48**(5): p. 640-6.
45. Kerr, E.M., et al., *Mutant Kras copy number defines metabolic reprogramming and therapeutic susceptibilities.* Nature, 2016. **531**(7592): p. 110-3.
46. Yuan, T.L., et al., *Differential Effector Engagement by Oncogenic KRAS.* Cell Rep, 2018. **22**(7): p. 1889-1902.
47. Jones, S., et al., *Core signaling pathways in human pancreatic cancers revealed by global genomic analyses.* Science, 2008. **321**(5897): p. 1801-6.
48. Amanam, I. and V. Chung, *Targeted Therapies for Pancreatic Cancer.* Cancers (Basel), 2018. **10**(2).
49. Collisson, E.A., et al., *Subtypes of pancreatic ductal adenocarcinoma and their differing responses to therapy.* Nat Med, 2011. **17**(4): p. 500-3.
50. Bailey, P., et al., *Genomic analyses identify molecular subtypes of pancreatic cancer.* Nature, 2016. **531**(7592): p. 47-52.
51. Birnbaum, D.J., et al., *Validation and comparison of the molecular classifications of pancreatic carcinomas.* Mol Cancer, 2017. **16**(1): p. 168.
52. Daemen, A., et al., *Metabolite profiling stratifies pancreatic ductal adenocarcinomas into subtypes with distinct sensitivities to metabolic inhibitors.* Proc Natl Acad Sci U S A, 2015. **112**(32): p. E4410-7.
53. Cameron, E. and A. Campbell, *The orthomolecular treatment of cancer. II. Clinical trial of high-dose ascorbic acid supplements in advanced human cancer.* Chem Biol Interact, 1974. **9**(4): p. 285-315.
54. Creagan, E.T., et al., *Failure of high-dose vitamin C (ascorbic acid) therapy to benefit patients with advanced cancer. A controlled trial.* N Engl J Med, 1979. **301**(13): p. 687-90.
55. Moertel, C.G., et al., *High-dose vitamin C versus placebo in the treatment of patients with advanced cancer who have had no prior chemotherapy. A randomized double-blind comparison.* N Engl J Med, 1985. **312**(3): p. 137-41.
56. Cameron, E. and A. Campbell, *Innovation vs. quality control: an 'unpublishable' clinical trial of supplemental ascorbate in incurable cancer.* Med Hypotheses, 1991. **36**(3): p. 185-9.
57. Padayatty, S.J., et al., *Vitamin C pharmacokinetics: implications for oral and intravenous use.* Ann Intern Med, 2004. **140**(7): p. 533-7.
58. Levine, M., et al., *Vitamin C pharmacokinetics in healthy volunteers: evidence for a recommended dietary allowance.* Proc Natl Acad Sci U S A, 1996. **93**(8): p. 3704-9.
59. Graumlich, J.F., et al., *Pharmacokinetic model of ascorbic acid in healthy male volunteers during depletion and repletion.* Pharm Res, 1997. **14**(9): p. 1133-9.
60. Welsh, J.L., et al., *Pharmacological ascorbate with gemcitabine for the control of metastatic and node-positive pancreatic cancer (PACMAN): results from a phase I clinical trial.* Cancer Chemother Pharmacol, 2013. **71**(3): p. 765-75.
61. Polireddy, K., et al., *High Dose Parenteral Ascorbate Inhibited Pancreatic Cancer Growth and Metastasis: Mechanisms and a Phase I/IIa study.* Sci Rep, 2017. **7**(1): p. 17188.

62. Monti, D.A., et al., *Phase I evaluation of intravenous ascorbic acid in combination with gemcitabine and erlotinib in patients with metastatic pancreatic cancer.* PLoS One, 2012. **7**(1): p. e29794.
63. Stephenson, C.M., et al., *Phase I clinical trial to evaluate the safety, tolerability, and pharmacokinetics of high-dose intravenous ascorbic acid in patients with advanced cancer.* Cancer Chemother Pharmacol, 2013. **72**(1): p. 139-46.
64. Hoffer, L.J., et al., *High-dose intravenous vitamin C combined with cytotoxic chemotherapy in patients with advanced cancer: a phase I-II clinical trial.* PLoS One, 2015. **10**(4): p. e0120228.
65. Hoffer, L.J., et al., *Phase I clinical trial of i.v. ascorbic acid in advanced malignancy.* Ann Oncol, 2008. **19**(11): p. 1969-74.
66. Blaschke, K., et al., *Vitamin C induces Tet-dependent DNA demethylation and a blastocyst-like state in ES cells.* Nature, 2013. **500**(7461): p. 222-6.
67. Agathocleous, M., et al., *Ascorbate regulates haematopoietic stem cell function and leukaemogenesis.* Nature, 2017. **549**(7673): p. 476-481.
68. Shenoy, N., et al., *Upregulation of TET activity with ascorbic acid induces epigenetic modulation of lymphoma cells.* Blood Cancer J, 2017. **7**(7): p. e587.
69. Knowles, H.J., et al., *Effect of ascorbate on the activity of hypoxia-inducible factor in cancer cells.* Cancer Res, 2003. **63**(8): p. 1764-8.
70. Vissers, M.C., et al., *Modulation of hypoxia-inducible factor-1 alpha in cultured primary cells by intracellular ascorbate.* Free Radic Biol Med, 2007. **42**(6): p. 765-72.
71. Kuiper, C., et al., *Intracellular ascorbate enhances hypoxia-inducible factor (HIF)-hydroxylase activity and preferentially suppresses the HIF-1 transcriptional response.* Free Radic Biol Med, 2014. **69**: p. 308-17.
72. Kuiper, C., et al., *Increased Tumor Ascorbate is Associated with Extended Disease-Free Survival and Decreased Hypoxia-Inducible Factor-1 Activation in Human Colorectal Cancer.* Front Oncol, 2014. **4**: p. 10.
73. Serrano, O.K., et al., *Antitumor effect of pharmacologic ascorbate in the B16 murine melanoma model.* Free Radic Biol Med, 2015. **87**: p. 193-203.
74. Chen, Q., et al., *Ascorbate in pharmacologic concentrations selectively generates ascorbate radical and hydrogen peroxide in extracellular fluid in vivo.* Proc Natl Acad Sci U S A, 2007. **104**(21): p. 8749-54.
75. Ma, Y., et al., *High-dose parenteral ascorbate enhanced chemosensitivity of ovarian cancer and reduced toxicity of chemotherapy.* Sci Transl Med, 2014. **6**(222): p. 222ra18.
76. Olney, K.E., et al., *Inhibitors of hydroperoxide metabolism enhance ascorbate-induced cytotoxicity.* Free Radic Res, 2013. **47**(3): p. 154-63.
77. Clement, M.V., et al., *The in vitro cytotoxicity of ascorbate depends on the culture medium used to perform the assay and involves hydrogen peroxide.* Antioxid Redox Signal, 2001. **3**(1): p. 157-63.
78. Cullen, J.J., *Ascorbate induces autophagy in pancreatic cancer.* Autophagy, 2010. **6**(3): p. 421-2.
79. Du, J., et al., *Mechanisms of ascorbate-induced cytotoxicity in pancreatic cancer.* Clin Cancer Res, 2010. **16**(2): p. 509-20.
80. Verrax, J. and P.B. Calderon, *Pharmacologic concentrations of ascorbate are achieved by parenteral administration and exhibit antitumoral effects.* Free Radic Biol Med, 2009. **47**(1): p. 32-40.

81. Doskey, C.M., et al., *Tumor cells have decreased ability to metabolize H2O2: Implications for pharmacological ascorbate in cancer therapy.* Redox Biol, 2016. **10**: p. 274-284.
82. Schoenfeld, J.D., et al., *O2(-) and H2O2-Mediated Disruption of Fe Metabolism Causes the Differential Susceptibility of NSCLC and GBM Cancer Cells to Pharmacological Ascorbate.* Cancer Cell, 2017. **31**(4): p. 487-500 e8.
83. Mayland, C.R., M.I. Bennett, and K. Allan, *Vitamin C deficiency in cancer patients.* Palliat Med, 2005. **19**(1): p. 17-20.
84. Fiaschi, A.I., et al., *Glutathione, ascorbic acid and antioxidant enzymes in the tumor tissue and blood of patients with oral squamous cell carcinoma.* Eur Rev Med Pharmacol Sci, 2005. **9**(6): p. 361-7.
85. Koong, A.C., et al., *Pancreatic tumors show high levels of hypoxia.* Int J Radiat Oncol Biol Phys, 2000. **48**(4): p. 919-22.
86. Semenza, G.L., *HIF-1: upstream and downstream of cancer metabolism.* Curr Opin Genet Dev, 2010. **20**(1): p. 51-6.
87. Yun, J., et al., *Vitamin C selectively kills KRAS and BRAF mutant colorectal cancer cells by targeting GAPDH.* Science, 2015. **350**(6266): p. 1391-6.
88. Townsend, D.M., K.D. Tew, and H. Tapiero, *The importance of glutathione in human disease.* Biomed Pharmacother, 2003. **57**(3-4): p. 145-55.
89. Pastore, A., et al., *Analysis of glutathione: implication in redox and detoxification.* Clin Chim Acta, 2003. **333**(1): p. 19-39.
90. Chen, P., et al., *Anti-cancer effect of pharmacologic ascorbate and its interaction with supplementary parenteral glutathione in preclinical cancer models.* Free Radic Biol Med, 2011. **51**(3): p. 681-7.
91. May, J.M., *Recycling of vitamin C by mammalian thioredoxin reductase.* Methods Enzymol, 2002. **347**: p. 327-32.
92. May, J.M., et al., *Vitamin C recycling and function in human monocytic U-937 cells.* Free Radic Biol Med, 1999. **26**(11-12): p. 1513-23.
93. Schnelldorfer, T., et al., *Glutathione depletion causes cell growth inhibition and enhanced apoptosis in pancreatic cancer cells.* Cancer, 2000. **89**(7): p. 1440-7.
94. Park, S., et al., *Vitamin C in Cancer: A Metabolomics Perspective.* Front Physiol, 2018. **9**: p. 762.
95. Liu, Y., et al., *Emerging regulatory paradigms in glutathione metabolism.* Adv Cancer Res, 2014. **122**: p. 69-101.
96. Zitka, O., et al., *Redox status expressed as GSH:GSSG ratio as a marker for oxidative stress in paediatric tumour patients.* Oncol Lett, 2012. **4**(6): p. 1247-1253.
97. Gamcsik, M.P., et al., *Glutathione levels in human tumors.* Biomarkers, 2012. **17**(8): p. 671-91.
98. Warburg, O., F. Wind, and E. Negelein, *The Metabolism of Tumors in the Body.* J Gen Physiol, 1927. **8**(6): p. 519-30.
99. Reichert, M., et al., *Isolation, culture and genetic manipulation of mouse pancreatic ductal cells.* Nat Protoc, 2013. **8**(7): p. 1354-65.
100. Ying, H., et al., *PTEN is a major tumor suppressor in pancreatic ductal adenocarcinoma and regulates an NF-kappaB-cytokine network.* Cancer Discov, 2011. **1**(2): p. 158-69.
101. Unni, A.M., et al., *Evidence that synthetic lethality underlies the mutual exclusivity of oncogenic KRAS and EGFR mutations in lung adenocarcinoma*. Elife, 2015. **4**: p. e06907.

102. Huang, L., et al., *Ductal pancreatic cancer modeling and drug screening using human pluripotent stem cell- and patient-derived tumor organoids.* Nat Med, 2015. **21**(11): p. 1364-71.
103. Chakrabarti, R., et al., *Vitamin A as an enzyme that catalyzes the reduction of MTT to formazan by vitamin C.* J Cell Biochem, 2000. **80**(1): p. 133-8.
104. TeSlaa, T. and M.A. Teitell, *Techniques to monitor glycolysis.* Methods Enzymol, 2014. **542**: p. 91-114.
105. Zhuang, Y., et al., *Mechanisms by which low glucose enhances the cytotoxicity of metformin to cancer cells both in vitro and in vivo.* PLoS One, 2014. **9**(9): p. e108444.
106. Breslin, S. and L. O'Driscoll, *Three-dimensional cell culture: the missing link in drug discovery.* Drug Discov Today, 2013. **18**(5-6): p. 240-9.
107. Sachs, N., et al., *A Living Biobank of Breast Cancer Organoids Captures Disease Heterogeneity.* Cell, 2018. **172**(1-2): p. 373-386 e10.
108. Weeber, F., et al., *Preserved genetic diversity in organoids cultured from biopsies of human colorectal cancer metastases.* Proc Natl Acad Sci U S A, 2015. **112**(43): p. 13308-11.
109. Boj, S.F., et al., *Organoid models of human and mouse ductal pancreatic cancer.* Cell, 2015. **160**(1-2): p. 324-38.
110. van de Wetering, M., et al., *Prospective derivation of a living organoid biobank of colorectal cancer patients.* Cell, 2015. **161**(4): p. 933-45.
111. Sachs, N. and H. Clevers, *Organoid cultures for the analysis of cancer phenotypes.* Curr Opin Genet Dev, 2014. **24**: p. 68-73.
112. Broutier, L., et al., *Culture and establishment of self-renewing human and mouse adult liver and pancreas 3D organoids and their genetic manipulation.* Nat Protoc, 2016. **11**(9): p. 1724-43.
113. Sharma, S.V., D.A. Haber, and J. Settleman, *Cell line-based platforms to evaluate the therapeutic efficacy of candidate anticancer agents.* Nat Rev Cancer, 2010. **10**(4): p. 241-53.
114. Roy, P., et al., *Organoids as preclinical models to improve intraperitoneal chemotherapy effectiveness for colorectal cancer patients with peritoneal metastases: Preclinical models to improve HIPEC.* Int J Pharm, 2017. **531**(1): p. 143-152.
115. Broutier, L., et al., *Human primary liver cancer-derived organoid cultures for disease modeling and drug screening.* Nat Med, 2017. **23**(12): p. 1424-1435.
116. Seino, T., et al., *Human Pancreatic Tumor Organoids Reveal Loss of Stem Cell Niche Factor Dependence during Disease Progression.* Cell Stem Cell, 2018. **22**(3): p. 454-467 e6.
117. Aref, A.R., et al., *Screening therapeutic EMT blocking agents in a three-dimensional microenvironment.* Integr Biol (Camb), 2013. **5**(2): p. 381-9.
118. Neoptolemos, J.P., et al., *Adjuvant chemotherapy with fluorouracil plus folinic acid vs gemcitabine following pancreatic cancer resection: a randomized controlled trial.* JAMA, 2010. **304**(10): p. 1073-81.
119. Cieslak, J.A. and J.J. Cullen, *Treatment of Pancreatic Cancer with Pharmacological Ascorbate.* Curr Pharm Biotechnol, 2015. **16**(9): p. 759-70.
120. Espey, M.G., et al., *Pharmacologic ascorbate synergizes with gemcitabine in preclinical models of pancreatic cancer.* Free Radic Biol Med, 2011. **50**(11): p. 1610-9.
121. Prior, I.A., P.D. Lewis, and C. Mattos, *A comprehensive survey of Ras mutations in cancer.* Cancer Res, 2012. **72**(10): p. 2457-67.

122. Pantsar, T., et al., *Assessment of mutation probabilities of KRAS G12 missense mutants and their long-timescale dynamics by atomistic molecular simulations and Markov state modeling.* PLoS Comput Biol, 2018. **14**(9): p. e1006458.
123. Mak, I.W., N. Evaniew, and M. Ghert, *Lost in translation: animal models and clinical trials in cancer treatment.* Am J Transl Res, 2014. **6**(2): p. 114-8.
124. Lai, I.L., et al., *Targeting the Warburg effect with a novel glucose transporter inhibitor to overcome gemcitabine resistance in pancreatic cancer cells.* Carcinogenesis, 2014. **35**(10): p. 2203-13.
125. Raez, L.E., et al., *A phase I dose-escalation trial of 2-deoxy-D-glucose alone or combined with docetaxel in patients with advanced solid tumors.* Cancer Chemother Pharmacol, 2013. **71**(2): p. 523-30.
126. Price, G.S., et al., *Pharmacokinetics and toxicity of oral and intravenous lonidamine in dogs.* Cancer Chemother Pharmacol, 1996. **38**(2): p. 129-35.
127. Baek, G., et al., *MCT4 defines a glycolytic subtype of pancreatic cancer with poor prognosis and unique metabolic dependencies.* Cell Rep, 2014. **9**(6): p. 2233-49.
128. Osthus, R.C., et al., *Deregulation of glucose transporter 1 and glycolytic gene expression by c-Myc.* J Biol Chem, 2000. **275**(29): p. 21797-800.

Appendices

Summary of figures

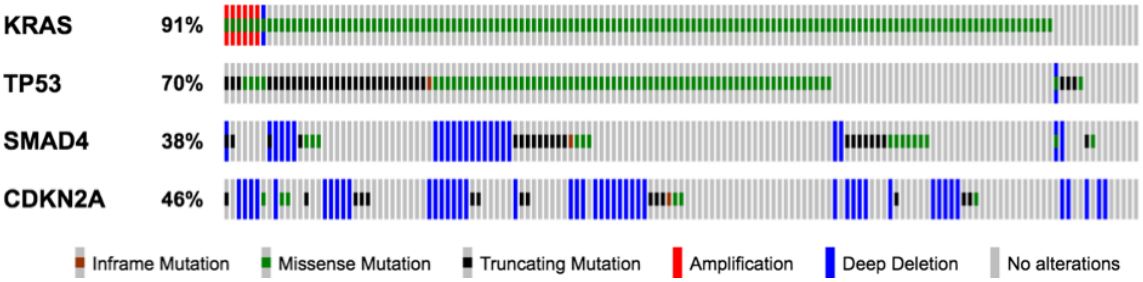

Figure 1.1: Rates of *KRAS*, *TP53*, *SMAD4*, and *CDKN2A* alterations in pancreatic ductal adenocarcinoma (PDAC)
Alteration rates and type in PDAC cases based on data from the Cancer Genome Atlas (TCGA) [34], figure generated in cBioPortal.

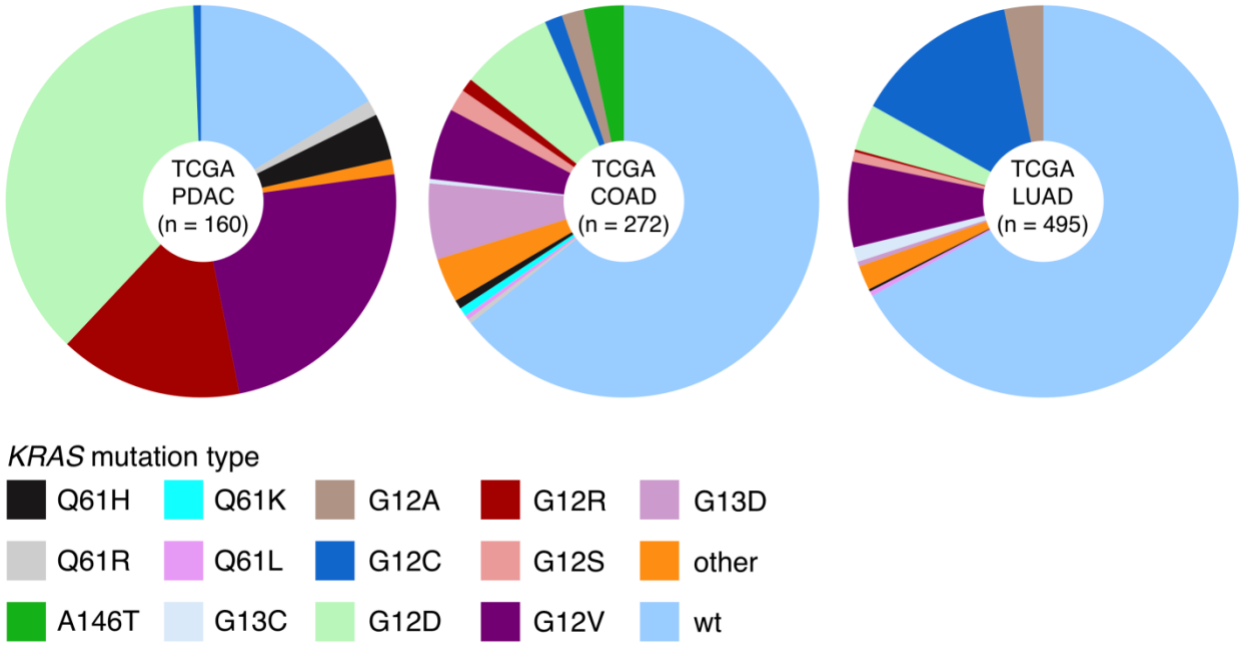

Figure 1.2: Proportion of KRAS mutations in pancreatic ductal adenocarcinoma (PDAC), colorectal cancer (COAD), and lung adenocarcinoma (LUAD)
Graphical representation of the proportion of KRAS mutation types and wild-type (wt) in PDAC, COAD, and LUAD from the Cancer Genome Atlas (TCGA) data [34]. Graph generated by James Topham using R.

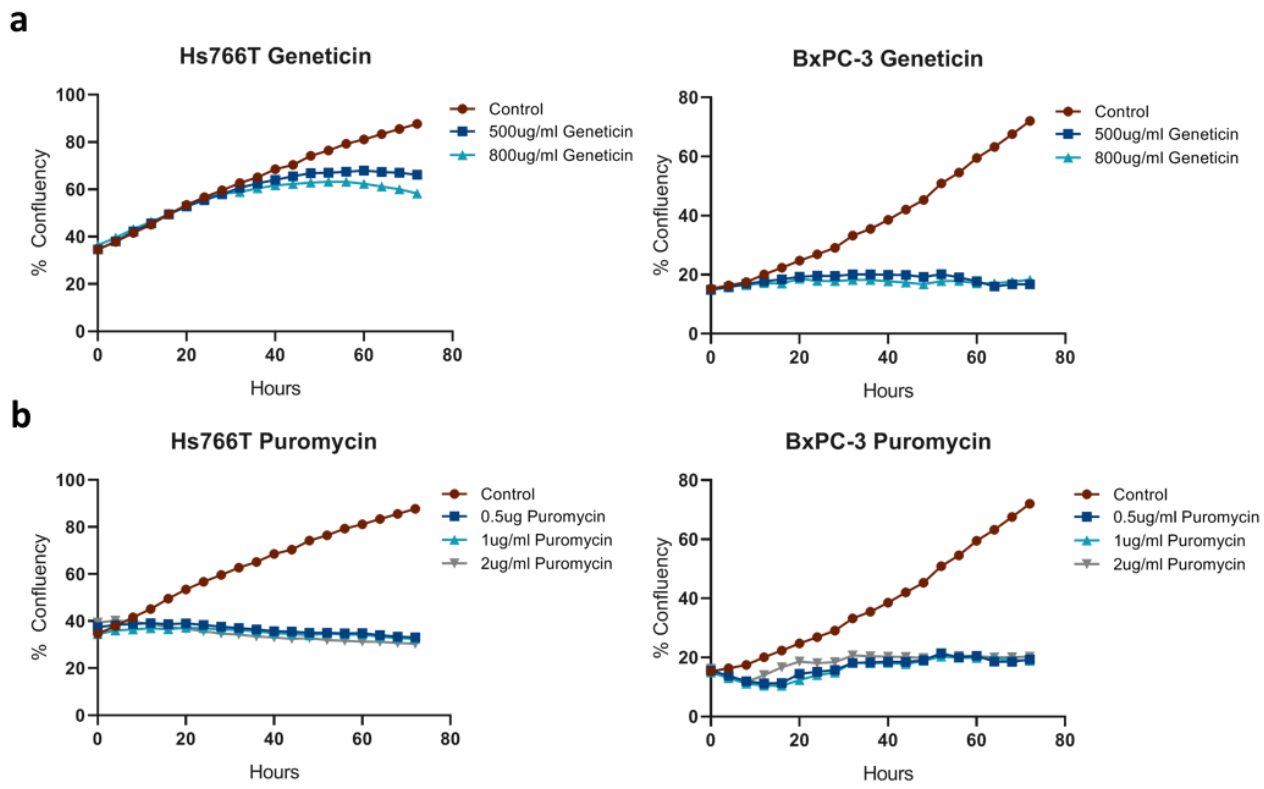

Figure 2.1: Antibiotic growth inhibition in Hs766T and BxPC-3
Cells were treated with geneticin **(a)**, puromycin **(b)** or control for 72 hours. Images were taken every 4 hours by IncuCyte ZOOM and confluency was determined using phase contrast analysis

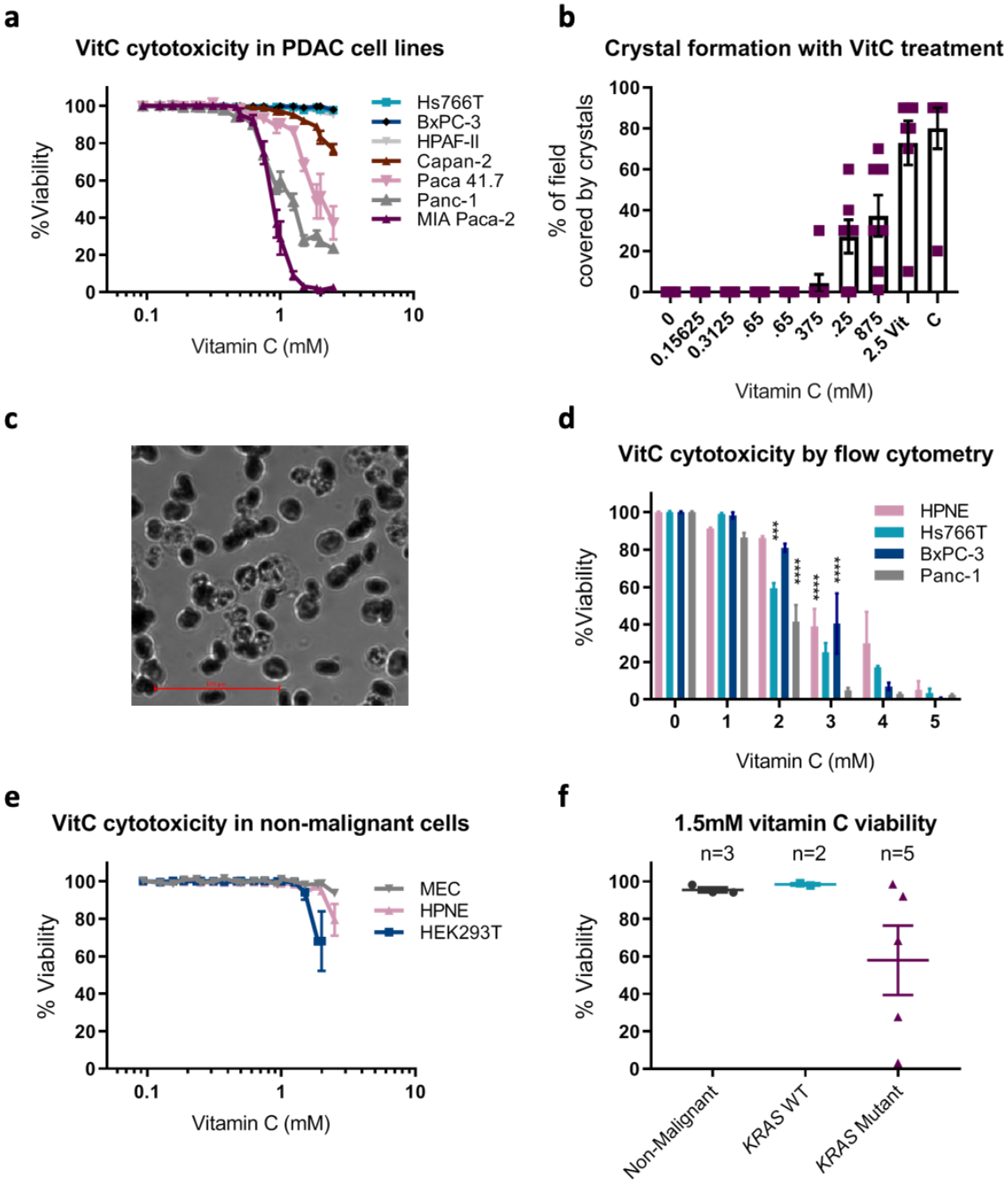

Figure 3.1: Vitamin C differential toxicity in PDAC cell lines
(**a**) Viability curves of PDAC cell lines after 24-hour treatment with vitamin C (VitC) (0-2.5mM) using IN Cell analysis. (**b**) Bar graph of estimated crystal formation after exposure to vitamin C (1-5mM) (**c**) Brightfield image of MIA Paca-2 cells treated with 2.5mM vitamin C (**d**)Viability bar graphs of PDAC and non-malignant HPNE cells treated with vitamin C (0-5mM) for 72 hours and stained with SYTOX Green to test for viability by flow cytometry. ***p<0.001, ****p<0.0001, compared to respective controls, two-way ANOVA Tukey's multiple comparisons test (**e**) Viability curves of non-malignant cell lines treated with vitamin C (0-2.5mM) for 24 hours tested with IN Cell analysis. ****p<0.0001, 1.5mM compared to control for HPNE and HEK, two-way ANOVA Tukey's multiple comparisons test (**f**) Plot of single dose (1.5mM) viability from data used for Figure3.1**a** segregated based on KRAS mutation.

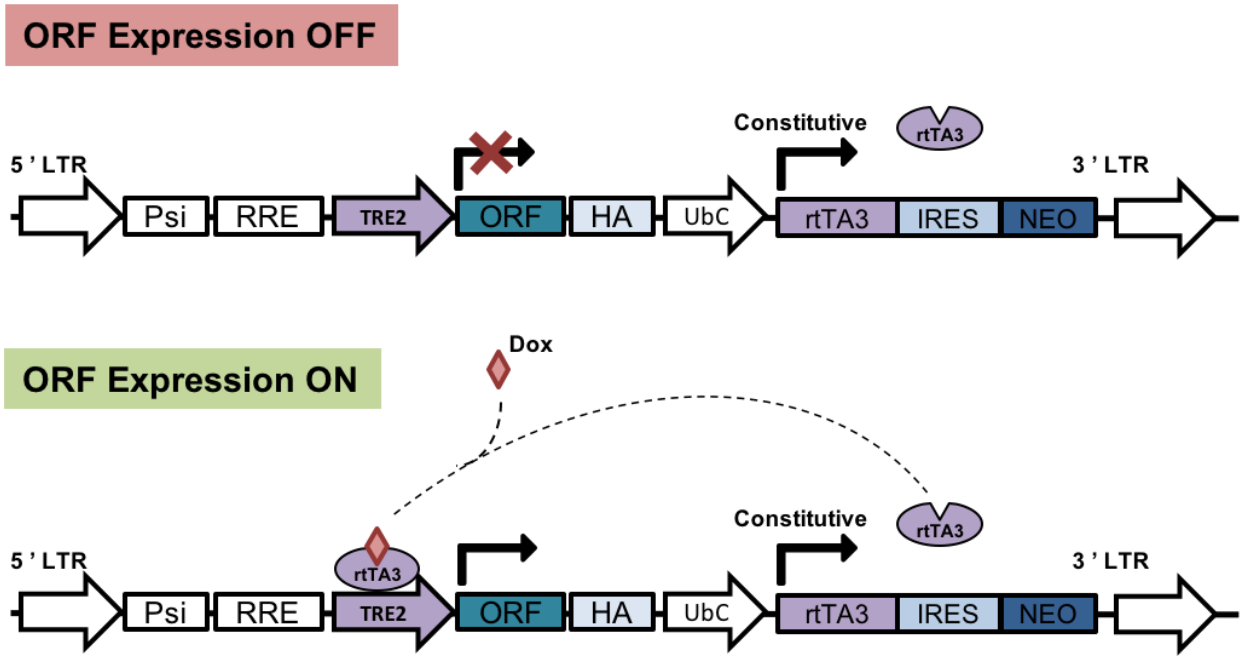

Figure 3.2: Diagram of TET-ON system for *KRAS* G12V model system
Doxycycline (Dox) is used to induce expression of the open reading frame (ORF) containing either *KRAS* G12D or *GFP*. Tetracycline transactivator (rTA3) is constitutively expressed, however on its own it is unable to bind to the tetracycline response element (TRE2) indicating expression of the ORF is "OFF".

When rTA3 is bound to tetracycline, or a derivative such as Dox, it can bind to TRE2 to turn the ORF expression "ON". Plasmid map based on Addgene pInducer20 (www.addgene.org/44012/)

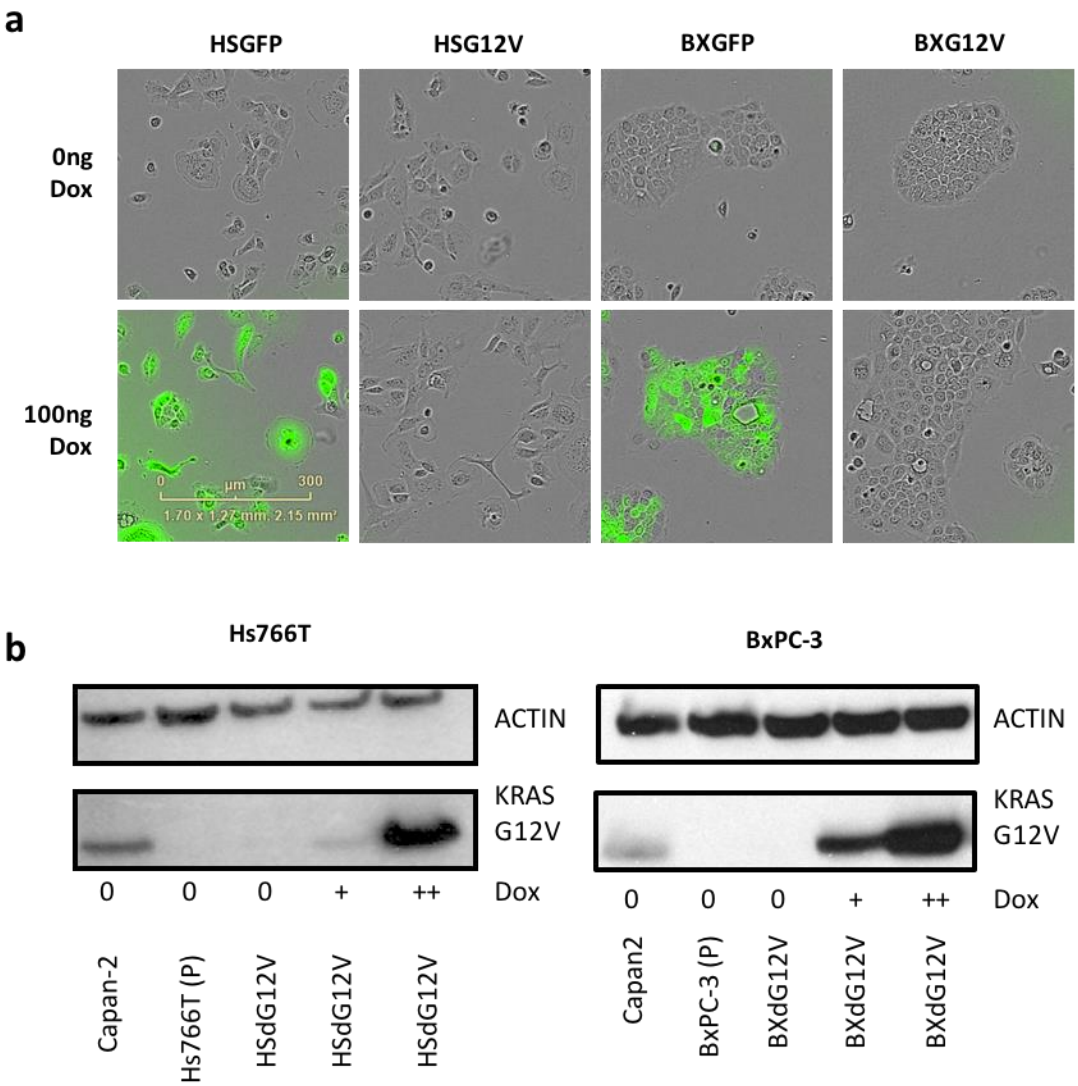

Figure 3.3: Expression validation of *KRAS* G12V model.
(**a**) Fluorescent microscopy images combined with brightfield (10X) of Dox-inducible *KRAS* G12V or *GFP* cell lines with 72 hour Dox exposure or control. (**b**) Presence of KRAS G12V was determined in Dox-inducible *KRAS* G12V cells after 72h of exposure to Dox (0-100ng) by western blot. B-actin was used as a loading control.

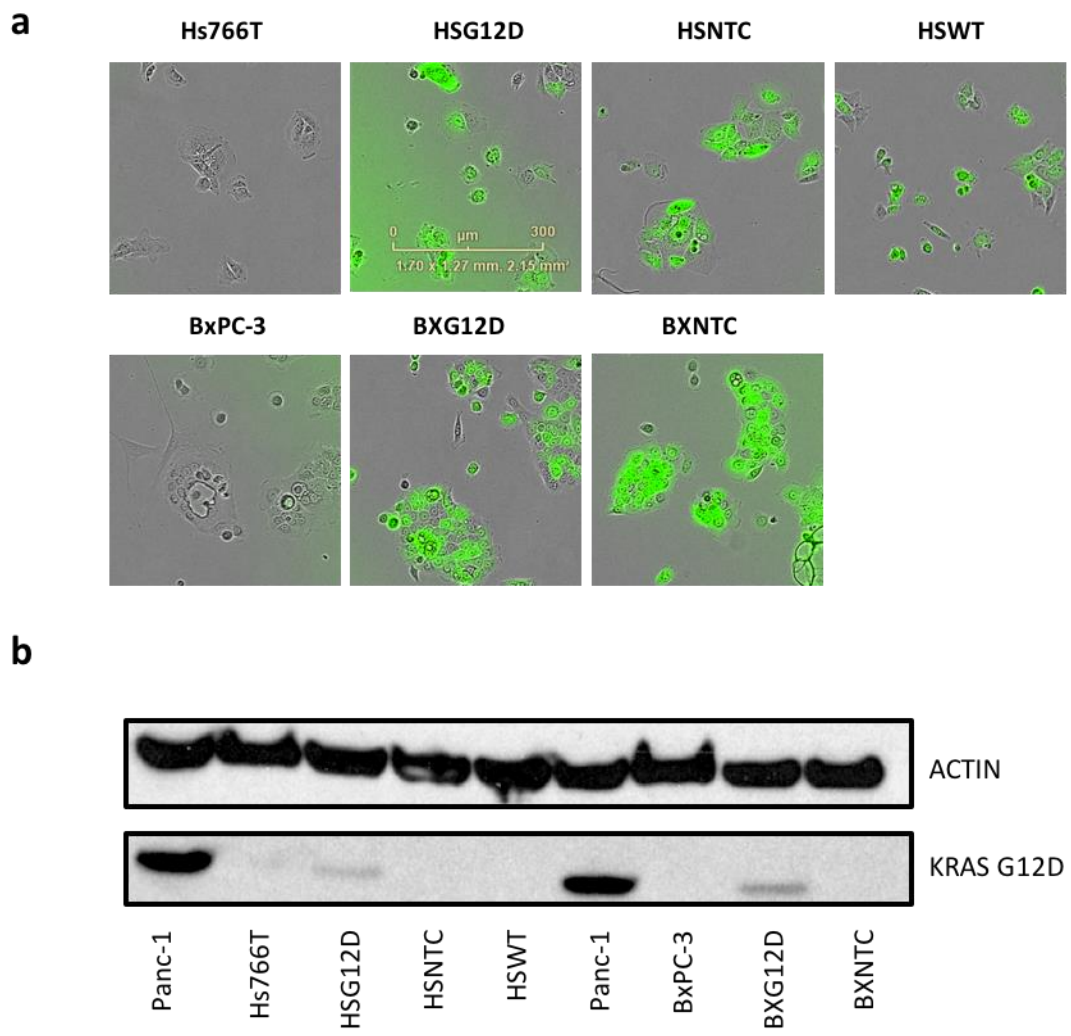

Figure 3.4: Expression validation of *KRAS* G12D model.
(**a**) Presence of GPF detected by fluorescent microscopy images combined with brightfield (10X) of parental and isogenic *KRAS* G12D, non-targetting control (NTC), and wildtype (WT) cells. (**b**) Western blot of *KRAS* G12D expression with loading control, ß-actin.

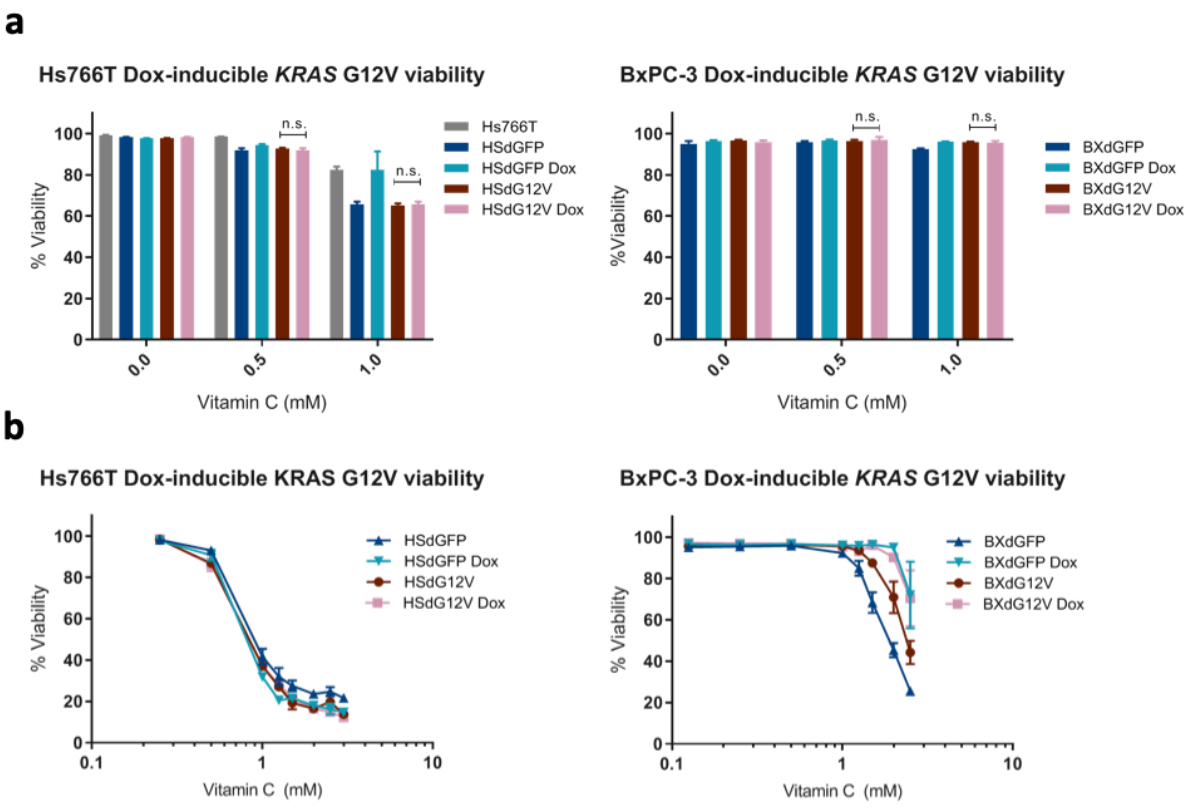

Figure 3.5: Vitamin C toxicity in Dox-inducible *KRAS* G12V cell lines
Viability results of control cells (Grey), GFP control (Blue), and *KRAS* G12V(Red) without expression (Dark shade) and with expression turned on by 72-hour exposure to Dox (Light shade). Cells were treated with (**a**) vitamin C (0-1mM) or (**b**) (0-2.5mM) for 24 hours.

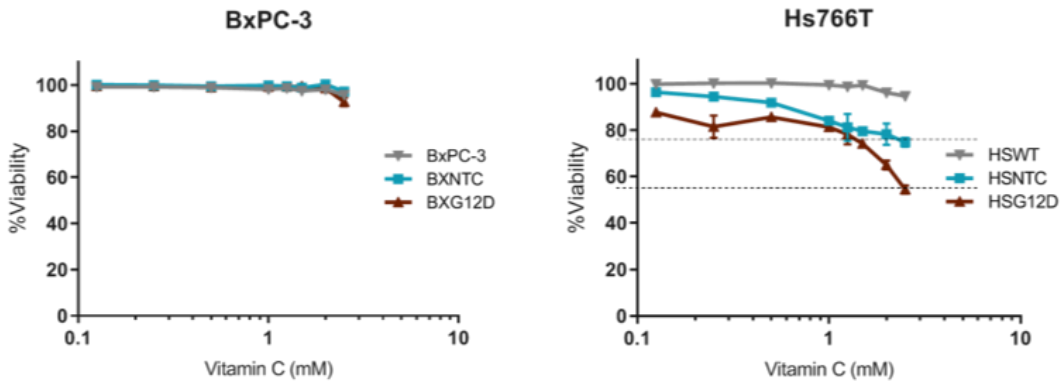

Figure 3.6: Vitamin C toxicity in *KRAS* G12D model system
Viability results of isogenic *KRAS* WT (Grey), NTC (Blue), or *KRAS* G12D (Red) cell lines treated with vitamin C (0-2.5mM) for 24 hours determined by IN Cell analysis. HSG12D vs HSNTC p=0.002 Wilcoxon matched pairs signed rank test.

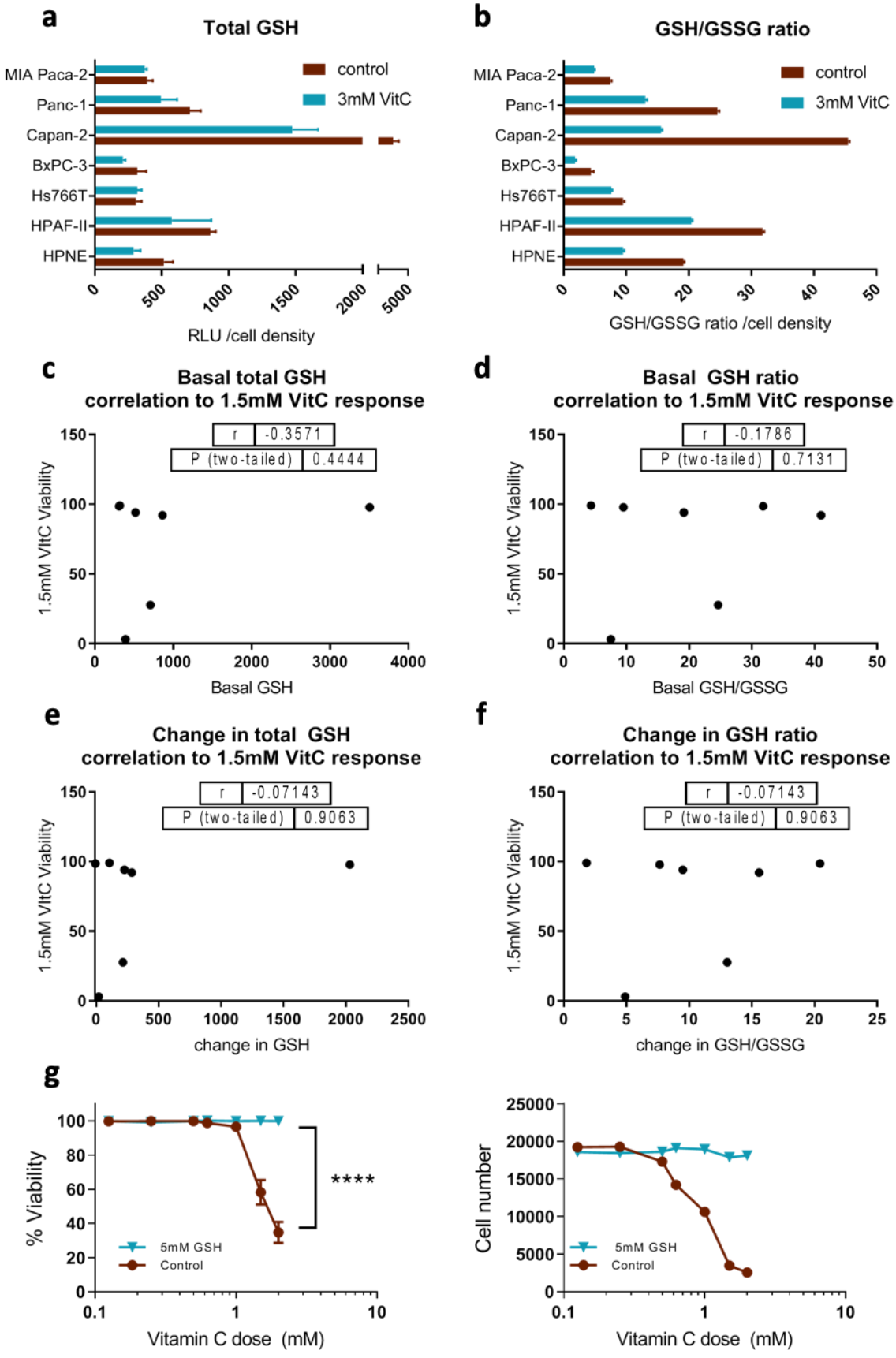
a
Total GSH
control
3mM VitC
MIA Paca-2
Panc-1
Capan-2
BxPC-3
Hs766T
HPAF-II
HPNE
0
500
1000
1500
2000
5000
RLU /cell density
b
GSH/GSSG ratio
control
3mM VitC
MIA Paca-2
Panc-1
Capan-2
BxPC-3
Hs766T
HPAF-II
HPNE
0
10
20
30
40
50
GSH/GSSG ratio /cell density
c
Basal total GSH
correlation to 1.5mM VitC response
r -0.3571
P (two-tailed) 0.4444
1.5mM VItC Viability
Basal GSH
d
Basal GSH ratio
correlation to 1.5mM VitC response
r -0.1786
P (two-tailed) 0.7131
1.5mM VItC Viability
Basal GSH/GSSG
e
Change in total GSH
correlation to 1.5mM VitC response
r -0.07143
P (two-tailed) 0.9063
1.5mM VItC Viability
change in GSH
f
Change in GSH ratio
correlation to 1.5mM VitC response
r -0.07143
P (two-tailed) 0.9063
1.5mM VItC Viability
change in GSH/GSSG
g
% Viability
****
5mM GSH
Control
Vitamin C dose (mM)
Cell number
5mM GSH
Control
Vitamin C dose (mM)

Figure 3.7: Cellular glutathione levels and relation to vitamin C toxicity.
(**a**) Bar plots indicating total glutathione (GSH) and (**b**) GSH/GSSG ratio of untreated (Blue) or 3mM vitamin C (VitC) for 2 hours (Blue) detected by luminescence and normalized to cell density. No correlation between 1.5mM vitamin C viability to (**c**) basal total GSH (rho=-0.3571, p=0.4444), (**d**) basal GSH/GSSG ratio (rho=-0.1786, p=0.7131), (**e)** change in total GSH with treatment (rho=-0.07143, p=0.9063), and (**f**) change in GSH/GSSG ratio with treatment (rho=-0.07143, p=0.9063) by spearman's correlations. (**g**) Viability and total cell number of MIA Paca-2 cells cultured in vitamin C (0-2mM) with and without 5mM GSH for 72 hours determined with IN Cell analyzer. Data was analyzed by two-way ANOVA (**** $p<0.0001$ for 1.5mM and 2mM vitamin C)

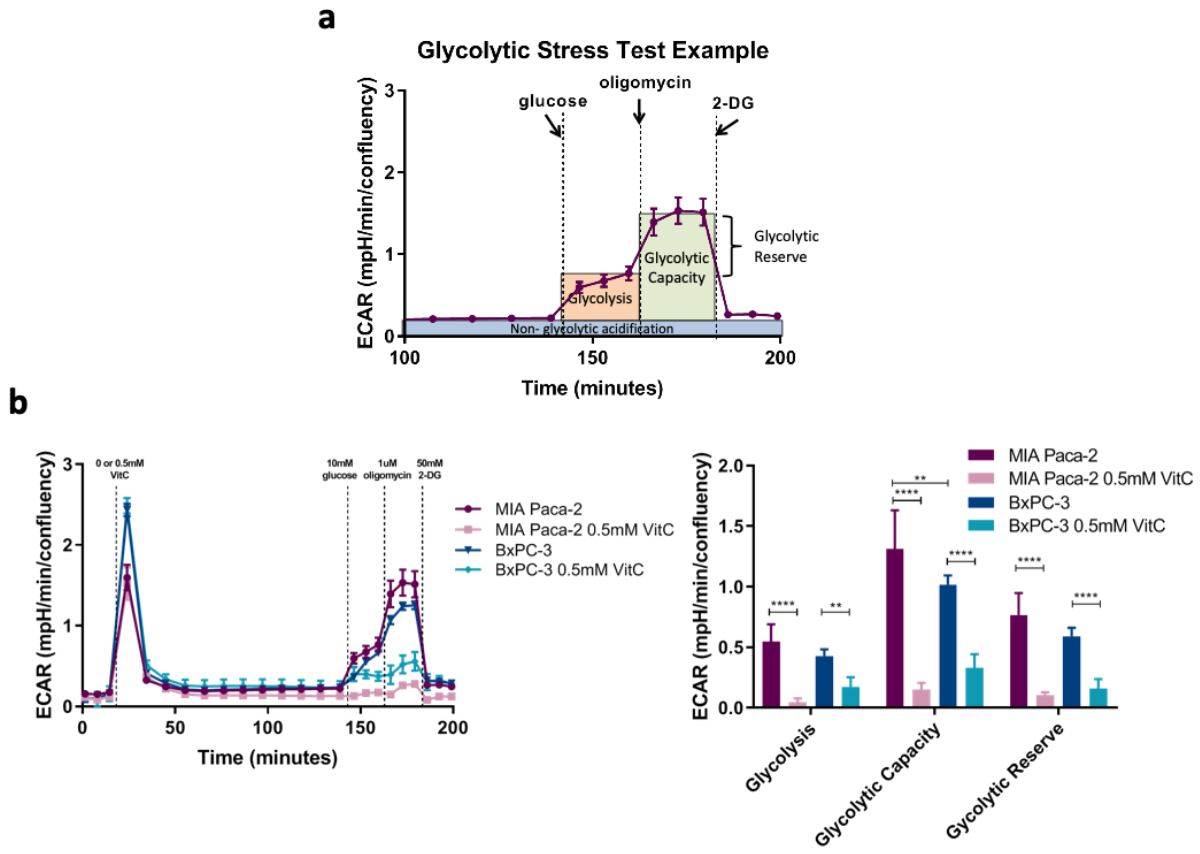

Figure 3.8: Changes in Glycolysis after vitamin C exposure.
Glycolysis was analyzed using Seahorse XFe96 glycolytic stress test. (**a**) Example of data and ranges where glycolysis, glycolytic capacity, and glycolytic reserve can be calculated. (**b**) Extracellular acidification rates (ECAR) of MIA Paca-2 and BxPC-3 of glycolytic stress test following 2-hour exposure to 0 or 0.5mM vitamin C (VitC) and normalized to well confluency determined by IncuCyte. Two-way ANOVA was used to analyze differences between treatments. ****$p < 0.0001$, **$p < 0.01$.

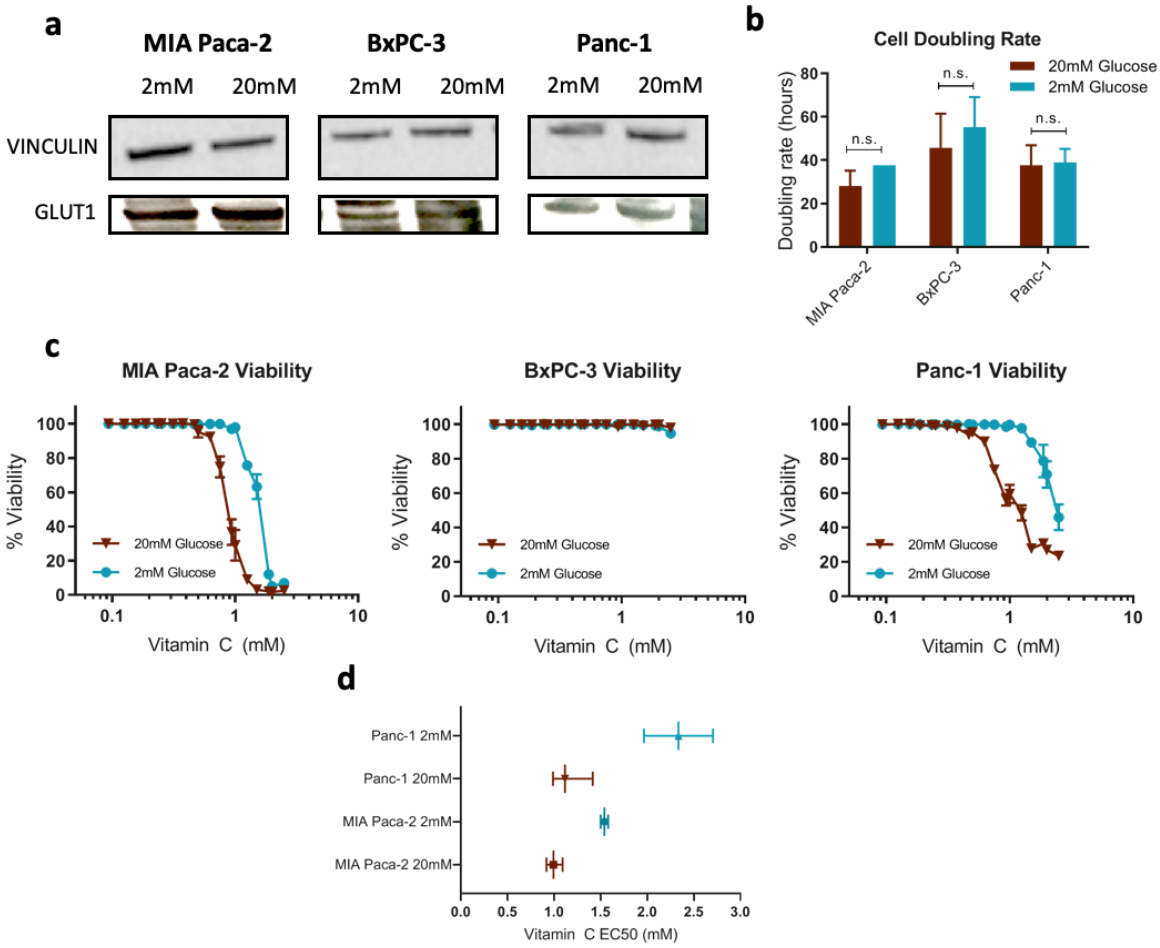

Figure 3.9: Effect of 2mM and 20mM glucose conditions on vitamin C toxicity and GLUT1 transporter.
(**a**) Western blot of GLUT1 in cell lines cultured in either 2mM or 20mM glucose containing media for 72 hours. (**b**) Bar plot indicating doubling rates of cell lines cultured in either for 72 hours in 2mM (Blue) and 20mM (Red) glucose containing media. Non-significant (N.S) based on 2-way ANOVA (**c**) Viability results of PDAC cells cultured in either 2mM (Blue) or 20mM (Red) containing media for 24 hours and subsequently treated with vitamin C (0-2.5mM). Viability was then determined through IN Cell analysis. (**d**) Viability EC50s determined using non-linear fit and plotted with 95% C.I.

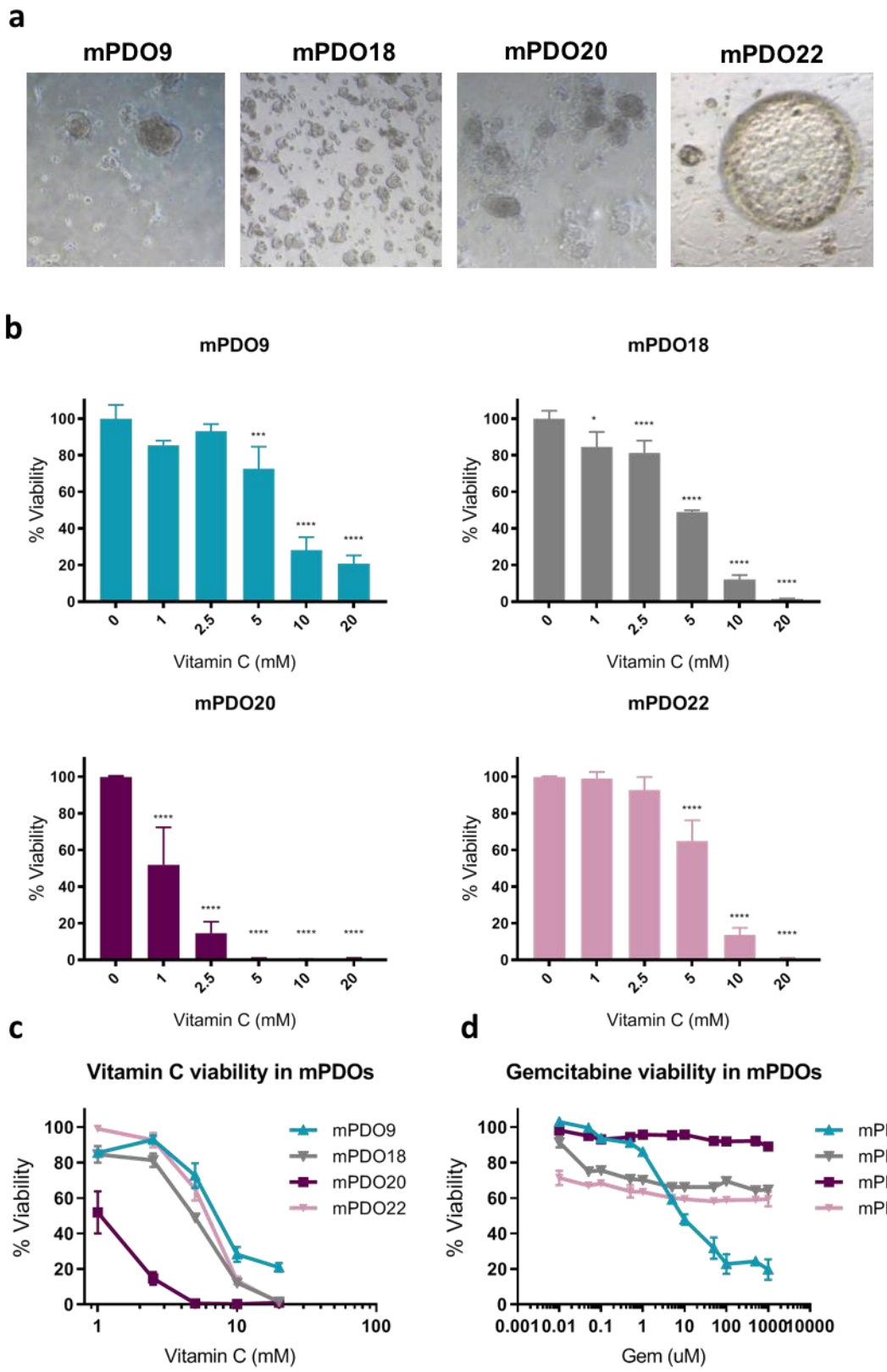
a
mPDO9
mPDO18
mPDO20
mPDO22
b
mPDO9
mPDO18
mPDO20
mPDO22
% Viability
Vitamin C (mM)
0
1
2.5
5
10
20
c
Vitamin C viability in mPDOs
mPDO9
mPDO18
mPDO20
mPDO22
Vitamin C (mM)
d
Gemcitabine viability in mPDOs
mPDO 9
mPDO18
mPDO20
mPDO22
Gem (uM)
0.001
0.01
0.1
1
10
100
1000
10000

Figure 3.10: Toxicity of vitamin C and Gemcitabine in PDOs.
(**a**) Cell viability results of organoids were treated with vitamin C (0-20mM) for 72 hours prior to IN Cell analysis. Viability normalized to untreated control. Differences in viability were compared to untreated controls by two-way ANOVA Tukey's multiple comparisons (*p<0.1, ***p<0.001, ****p<0.0001). (**b**) Cell viability results of xPDO41 treated with vitamin C (1-20mM) either alone or in combination with gemcitabine (Gem) for 72 hours prior to staining and analysis. Viability was normalized to untreated control. Differences in viability were compared to respective vitamin C untreated controls by two-way ANOVA Tukey's multiple comparisons. (**c**) Viability of organoids treated with Gem (0-1mM) for 72 hours prior to staining and IN Cell analysis. Viability was normalized to vehicle control.

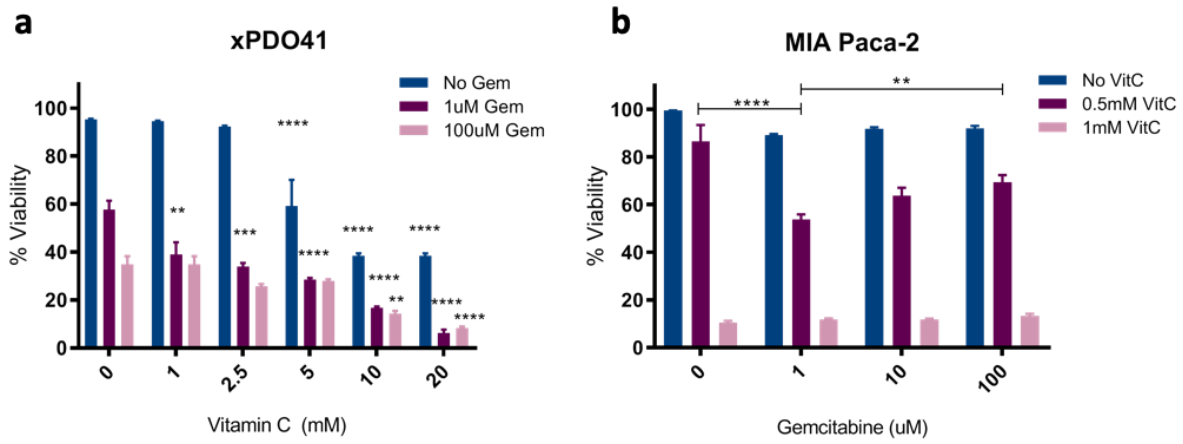

Figure 3.11: Combination treatment of vitamin C and gemcitabine
(**a**) Cell viability results of xPDO41 treated with vitamin C (1-20mM) either alone or in combination with gemcitabine (Gem) for 72 hours prior to staining and analysis. Viability was normalized to untreated control. Differences in viability were compared to respective vitamin C untreated controls by two-way ANOVA Tukey's multiple comparisons. (**b**) Cell viability results of MIA Paca-2 treated with gemcitabine (0-100µM) either alone or in combination with vitamin C (VitC) for 72 hours prior to staining and analysis. Viability was normalized to untreated control. Differences in viability were compared by two-way ANOVA Tukey's multiple comparisons. (*p<0.1, **p<0.01) ***p<0.001, ****p<0.0001